

Accepted Manuscript

Research paper

A new magnetically recyclable heterogeneous palladium(II) as a green catalyst for Suzuki-Miyaura cross-coupling and reduction of nitroarenes in aqueous medium at room temperature

Vishal Kandathil, Tuhin S. Koley, K. Manjunatha, Ramesh B. Dateer, Rangappa S. Keri, B.S. Sasidhar, Shivaputra A. Patil, Siddappa A. Patil

PII: S0020-1693(17)31746-2
DOI: <https://doi.org/10.1016/j.ica.2018.04.015>
Reference: ICA 18206

To appear in: *Inorganica Chimica Acta*

Received Date: 13 November 2017
Revised Date: 1 March 2018
Accepted Date: 10 April 2018

Please cite this article as: V. Kandathil, T.S. Koley, K. Manjunatha, R.B. Dateer, R.S. Keri, B.S. Sasidhar, S.A. Patil, S.A. Patil, A new magnetically recyclable heterogeneous palladium(II) as a green catalyst for Suzuki-Miyaura cross-coupling and reduction of nitroarenes in aqueous medium at room temperature, *Inorganica Chimica Acta* (2018), doi: <https://doi.org/10.1016/j.ica.2018.04.015>

This is a PDF file of an unedited manuscript that has been accepted for publication. As a service to our customers we are providing this early version of the manuscript. The manuscript will undergo copyediting, typesetting, and review of the resulting proof before it is published in its final form. Please note that during the production process errors may be discovered which could affect the content, and all legal disclaimers that apply to the journal pertain.



A new magnetically recyclable heterogeneous palladium(II) as a green catalyst for Suzuki-Miyaura cross-coupling and reduction of nitroarenes in aqueous medium at room temperature

Vishal Kandathil^{at}, Tuhin S. Koley^{at}, Manjunatha K^a, Ramesh B. Dateer^a, Rangappa S. Keri^a, Sasidhar B. S.^b, Shivaputra A. Patil^c, Siddappa A. Patil^{a,*}

^a*Centre for Nano and Material Sciences, Jain University, Jain Global Campus, Kanakapura, Ramanagaram, Bangalore 562112, India.*

^b*Organic Chemistry Section, Chemical Sciences & Technology Division, National Institute for Interdisciplinary Science and Technology (CSIR), Thiruvananthapuram - 695019, Kerala, India.*

^c*Pharmaceutical Sciences Department, College of Pharmacy, Rosalind Franklin University of Medicine and Science, 3333 Green Bay Road, North Chicago, IL 60064, USA.*

*Corresponding author: Dr. Siddappa A. Patil

Tel: +91 80 27577254

Fax: +91 80 27577211

E-mail: p.siddappa@jainuniversity.ac.in

[†]These authors contributed equally.

Abstract

In the current work, a new stable and powerful magnetic nanoparticle supported Schiff base-palladium(II) (MNPs@SB-Pd) nanomagnetic catalyst was synthesized. The structural feature of the MNPs@SB-Pd nanomagnetic catalyst was properly characterized using a combination of attenuated total reflectance infrared spectroscopy (ATR-IR), ultraviolet-visible spectroscopy (UV-Visible), inductively coupled plasma-atomic emission spectroscopy (ICP-AES), energy-dispersive X-ray spectroscopy (EDS), field-emission scanning electron microscopy (FESEM), transmission electron microscopy (TEM), X-ray powder diffraction (XRD), thermogravimetric analysis (TGA) and Brunauer-Emmett-Teller surface area analysis (BET). The air- and moisture stable prepared MNPs@SB-Pd nanomagnetic catalyst was applied in C-C bond formation through Suzuki-Miyaura cross-coupling reactions and reduction of nitroarenes. Use of green medium, eco-friendly, waste-free, efficient preparation leading to high yield of products, short reaction time and cost effective catalyst are the major benefits of the method presented. In addition, the MNPs@SB-Pd nanomagnetic catalyst was easily separated from the reaction mixture with the help of an external magnetic field and reused for five consecutive cycles in Suzuki-Miyaura cross-coupling and ten consecutive cycles in reduction of nitroarene reactions with no significant loss of catalytic efficiency.

Keywords: Magnetic nanoparticle; Schiff base-palladium(II); nanomagnetic catalyst; synthesis and characterization; Suzuki-Miyaura cross-coupling; reduction of nitroarenes

1. Introduction

The palladium catalysed Suzuki-Miyaura cross-coupling reactions are probably among the most commonly employed approaches of C-C bond formation in organic transformations [1-3]. They have been used for the synthesis of various organic compounds, especially those of pharmaceutical drugs, agrochemicals, supramolecular chemistry, complex natural products, and engineering materials such as liquid crystals, molecular wires and conducting polymers [4-8]. Hence, many efforts have been made to the development of homogeneous systems for Suzuki-Miyaura cross-coupling reaction, such as N-heterocyclic carbenes, oxime palladacycles, diazabutadienes, amines and phosphine ligands [9-12]. On the other hand, complete reduction of nitroarenes to aromatic amines is very much essential, as they are important intermediates for the preparation of agriculture products, rubber chemicals, photographic chemicals, pharmaceuticals, polyureathens and polymers [13-15]. The traditional methods to synthesize amines are based on the amination of numerous functional groups such as H, F, Cl, Br, I, OH, etc. through the corresponding diazonium salts [16] or the reduction of nitro compounds with homogeneous catalysts [17-20]. However, major drawback of homogeneous catalysts is the difficulty of their recovery from the reaction medium for reuse. This problem is of environmental and economic concern in large-scale syntheses. Recent past, Schiff base transition metal complexes have been successfully used as catalyst for various organic reactions [21, 22]. Stable Schiff base transition metal complexes have been easily synthesized from many transition metal ions with different oxidation states. In many cases, Schiff base transition metal complexes have been anchored on different materials, such as dendrimers, polymers, silica, and zeolites [23-26]. However,

inorganic matrices show some advantages compared to organic supports such as high thermal, chemical, and mechanical stability [27-30].

In this regard, magnetic nanoparticles supported catalysts were successfully used as heterogeneous catalysts. The main benefits of magnetic nanoparticles supported catalyst is that nanoparticles can be efficiently separated from the reaction mixture by using an external magnet after completion of the reaction and easily reused for next round [31-35]. In addition, magnetic nanoparticles supported catalysts also exhibit high dispersion and reactivity with high chemical stability. These advantages of magnetic nanoparticles make them superior over other supporting materials for immobilization of many catalysts and ligands on these nanoparticles [36]. Therefore, magnetic nanoparticles supported catalytic systems have been successfully applied as potent, clean and environment friendly recoverable nanomagnetic catalysts for many organic reactions.

Our continued interest in this area led us to explore the magnetic nanoparticles supported Schiff base palladium(II) complex, which can be suitably applied for Suzuki-Miyaura cross-coupling and reduction of nitroarenes reactions in aqueous (eco-friendly) medium at room temperature, and then could be easily separated from the product to reuse. Herein, we report the synthesis and characterization of a new magnetic nanoparticle supported Schiff base-palladium(II) nanomagnetic catalyst for Suzuki-Miyaura cross-coupling of various aryl bromides/chlorides/iodides with phenylboronic acid and reduction of nitroarenes reactions. The MNPs@SB-Pd nanomagnetic catalyst was structurally characterized by the combination of spectroscopic and microscopic techniques. Furthermore, MNPs@SB-Pd nanomagnetic catalyst is shown to exhibit high catalytic activity in both Suzuki-Miyaura cross-coupling and reduction of nitroarenes reactions.

2. Experimental procedures

2.1. Materials

All solvents were purified according to standard methods prior to use. Unless otherwise stated, all reactions were performed under aerobic conditions in oven-dried glassware with magnetic stirring. $\text{FeCl}_3 \cdot 6\text{H}_2\text{O}$, $\text{FeCl}_2 \cdot 4\text{H}_2\text{O}$, ammonium hydroxide, 2-hydroxy-3-methoxybenzaldehyde, 3-aminopropyl triethoxysilane, palladium(II) acetate, aryl halides, bases and phenylboronic acid were purchased from Sigma-Aldrich chemical company and were used without further purification. Heating was accomplished by either a heating mantle or silicone oil bath. Column chromatography was conducted on Silica gel 230-400 mesh (Merck) and preparative thin-layer chromatography was carried out using 0.25 mm Merck TLC silica gel plates with UV light as a visualizing agent. Yields refer to chromatographically pure material. Concentration in vacuo refers to the removal of volatile solvent using a rotary evaporator attached to a dry diaphragm pump (10-15 mm Hg) followed by pumping to a constant weight with an oil pump (<300 mTorr). All the organic products were known and identified by comparison of their physical and spectral data with those of authentic samples.

2.2. Characterization

Attenuated total reflectance infrared spectra were recorded with Bruker Alpha Eco-ATR spectrometer. UV-visible spectrophotometry was carried out by SHIMADZU UV-1800 A11454907691. Brunauer-Emmett-Teller surface areas were obtained by physisorption of N_2 using Microtrac BELSORP MAX instrument. The elemental palladium content of the nanomagnetic catalyst was determined by Thermo Electron IRIS INTREPID II XSP DUO inductively coupled plasma-atomic emission spectroscopy. Transmission electron microscope

images were obtained using Jeol/JEM 2100 microscope. FESEM images along with energy dispersive X-ray spectroscopy to observe morphology and elemental distributions respectively were obtained with JEOL Model-JSM7100F. Thermogravimetric analysis was carried out by Perkin Elmer, Diamond TG/DTA with a heating rate of 10.0 °C/min. X-ray powder diffractometer patterns were obtained using Bruker AXS D8 Advance. ¹H NMR spectra were recorded at 400 MHz, and are reported relative to CDCl₃ (δ 7.27). ¹H NMR coupling constants (J) are reported in Hertz (Hz) and multiplicities are indicated as follows: s (singlet), d (doublet), t (triplet), m (multiplet). Liquid chromatography mass spectra (LC-MS) were recorded on Agilent technologies quadrupole LC-MS system.

2.3. Syntheses

2.3.1. Synthesis of hydroxyl substituted magnetic nanoparticles (MNPs) (1)

Hydroxyl substituted magnetic nanoparticles (**1**) were prepared by chemical co-precipitation of ferric and ferrous salts according to the reported method with slight modification. To a solution of FeCl₃·6H₂O (9.4 g, 34.77 mmol) in deionized water (100 mL) was added FeCl₂·4H₂O (3.46 g, 17.40 mmol). The reaction mixture was stirred for 30 minutes at 85 °C. Then, ammonium hydroxide (20 mL) solution was added drop wise to the reaction mixture with vigorous stirring at 85 °C to produce black colored precipitate and stirring was continued for additional 30 minutes. The black colored precipitate was separated by a permanent magnet and washed with deionized water until pH neutral. Finally, hydroxyl substituted magnetic nanoparticles were washed with ethanol (3 x 20 mL) and dried at 45-50 °C for 8 h.

2.3.2. Synthesis of amine functionalized magnetic nanoparticles (AFMNPs) (3)

Hydroxyl substituted magnetic nanoparticles (**1**) (4.0 g) were dispersed in ethanol (EtOH)-water (H₂O) (2:1) mixture (140 mL) with ultrasonication for 10 minutes. (3-

Aminopropyl)triethoxysilane (**2**) (15.2 g, 68.6 mmol) was added to the suspension and stirred at 45 °C for 24 h [37, 38]. Subsequently, the reaction mixture was cooled to room temperature. The dark brown amine-functionalized magnetic nanoparticles (**3**) were collected using magnetic separator, washed with deionized H₂O (3 x 20 mL) followed by ethanol (EtOH) (3 x 20 mL) and dried at 45 °C for 12 h.

2.3.3. *Synthesis of magnetic nanoparticle tethered Schiff base (MNP@SB) (5)*

To a suspension of aminofunctionalized magnetic nanoparticles (**3**) (4.0 g) in EtOH (60 mL) was added 2-hydroxy-3-methoxybenzaldehyde (**4**) (4.0 g, 26.28 mmol). The reaction mixture stirred at 70 °C for 24 h and then cooled to room temperature. The dark brown colored magnetic nanoparticle tethered Schiff base (**5**) was separated using an external magnetic field and washed with methanol (MeOH) (3 x 20 mL) and dried at 45 °C for 12 h.

2.3.4. *Synthesis of magnetic nanoparticle tethered Schiff base palladium(II) complex (MNP@SB-Pd) nanomagnetic catalyst (6)*

Palladium (II) acetate (0.87g, 3.87 mmol) was added to the solution of magnetic nanoparticle tethered Schiff base (**5**) (3.5 g) in EtOH (40 mL) and stirred at 70 °C for 12 h. Then the reaction mixture was cooled to room temperature. The MNP@SB-Pd nanomagnetic catalyst (**6**) as dark brown colored solid was isolated by an external magnet, washed with H₂O (3 x 20 mL) followed by EtOH (3 x 20 mL) and dried at 70 °C for 6 h.

2.3.5. *General procedure for Suzuki-Miyaura cross-coupling reactions catalyzed by MNP@SB-Pd nanomagnetic catalyst*

An oven-dried flask was charged with aryl halide (0.27 mmol), phenylboronic acid (0.036 g, 0.30 mmol), MNP@SB-Pd nanomagnetic catalyst (0.05 mol% Pd) and K₂CO₃ (0.082 g, 0.60 mmol). EtOH:H₂O (1:1, 10 mL) was added and the reaction mixture was stirred at room

temperature for designated time. The progress of the reaction was monitored using TLC. Then the reaction mixture was allowed to cool to room temperature and quenched by adding dichloromethane (20 mL) and the MNPs@SB-Pd nanomagnetic catalyst was separated using a permanent magnet. Dichloromethane layer was separated from water layer through separatory funnel and dried with anhydrous MgSO_4 . The dried dichloromethane layer was concentrated in vacuum and purified through column chromatography using hexane and ethyl acetate as eluting solvent to get the corresponding products in excellent yields.

1. *4-Nitrobiphenyl* (Table 5, entry 1): Pale yellow crystals. Melting point = 111-114 °C; ^1H NMR (400 MHz, CDCl_3): δ (ppm) = 7.42-7.50 (m, 3H), 7.65 (d, $J = 6.0$ Hz, 2H), 7.75 (d, $J = 6.8$ Hz, 2H), 8.28 (d, $J = 6.8$ Hz, 2H). LC-MS for $\text{C}_{12}\text{H}_9\text{NO}_2$: $m/z = 200.05$ $[\text{M}+\text{H}]^+$.

2. *2-Phenylbenzaldehyde* (Table 5, entry 2): Yellow oil. ^1H NMR (400 MHz, CDCl_3): δ (ppm) = 9.92 (s, 1H), 7.34-7.32 (m, 3H), 7.39-7.36 (m, 2H), 7.55 (d, $J = 7.6$ Hz, 2H), 7.71-7.75 (m, 2H). LC-MS for $\text{C}_{13}\text{H}_{10}\text{O}$: $m/z = 183.03$ $[\text{M}+\text{H}]^+$.

3. *4-Phenylbenzaldehyde* (Table 5, entry 3): Yellow crystals. Melting point = 57-58 °C; ^1H NMR (400 MHz, CDCl_3): δ (ppm) = 9.97 (s, 1H), 7.44-7.41 (m, 3H), 7.56 (d, $J = 8.0$ Hz, 2H), 7.70 (d, $J = 8.0$ Hz, 2H), 7.91 (d, $J = 8.0$ Hz, 2H). LC-MS for $\text{C}_{13}\text{H}_{10}\text{O}$: $m/z = 183.07$ $[\text{M}+\text{H}]^+$.

4. *4-Acetylbiphenyl* (Table 5, entries 4 and 16): White powder. Melting point = 119-121 °C; ^1H NMR (400 MHz, CDCl_3): δ (ppm) = 2.62 (s, 3H), 7.38-7.40 (m, 1H), 7.44-7.47 (m, 2H), 7.62 (d, $J = 7.6$ Hz, 2H), 7.66 (d, $J = 8.8$ Hz, 2H), 8.02 (d, $J = 8.4$ Hz, 2H). LC-MS for $\text{C}_{14}\text{H}_{12}\text{O}$: $m/z = 197.15$ $[\text{M}+\text{H}]^+$.

5. *Biphenyl* (Table 5, entries 5 and 17): Colorless crystals. Melting point = 68-71 °C; ^1H NMR (400 MHz, CDCl_3): δ (ppm) = 7.33 (t, $J = 7.6$ Hz, 2H), 7.45 (t, $J = 7.6$ Hz, 4H), 7.54 (d, $J = 8.0$ Hz, 4H). LC-MS for $\text{C}_{12}\text{H}_{10}$: $m/z = 155.06$ $[\text{M}+\text{H}]^+$.

6. *4-Methylbiphenyl* (Table 5, entries 6 and 18): White crystalline solid. Melting point = 45-48 °C; ^1H NMR (400 MHz, CDCl_3): δ (ppm) = 2.25 (s, 3H), 7.26-7.30 (m, 2H), 7.35-7.38 (m, 4H), 7.65 (s, 1H), 7.79 (d, $J = 7.6$ Hz, 2H). LC-MS for $\text{C}_{13}\text{H}_{12}$: $m/z = 169.07$ $[\text{M} + \text{H}]^+$.

7. *4-Aminobiphenyl* (Table 5, entry 7): Purple crystals. Melting point = 52-55 °C; ^1H NMR (400 MHz, CDCl_3): δ (ppm) = 7.51 (d, $J = 8.4$ Hz, 2H), 7.44-7.41 (m, 4H), 7.28-7.24 (m, 1H), 6.76 (d, $J = 8.0$ Hz, 2H), 3.70 (s, 2H). LC-MS for $\text{C}_{12}\text{H}_{11}\text{N}$: $m/z = 170.02$ $[\text{M}+\text{H}]^+$.

8. *4-Phenylbenzoic acid* (Table 5, entry 8): White solid. Melting point = 220-223 °C; ^1H NMR (400 MHz, CDCl_3): δ (ppm) = 7.35-7.37 (m, 4H), 7.44-7.41 (m, 1H), 7.54-7.51 (m, 3H), 7.65 (d, $J = 7.2$ Hz, 1H). LC-MS for $\text{C}_{13}\text{H}_{10}\text{O}_2$: $m/z = 199.12$ $[\text{M} + \text{H}]^+$.

9. *3-Phenylbenzoic acid* (Table 5, entry 9): Off-white crystals. Melting point = 163–165 °C; ¹H NMR (400 MHz, CDCl₃): δ (ppm) = 7.39–7.36 (m, 2H), 7.47–7.40(m, 1H), 7.62 (d, *J* = 7.2 Hz, 3H), 7.74 (d, *J* = 7.6 Hz, 2H), 7.86 (d, *J* = 7.2 Hz, 1H). LC-MS for C₁₃H₁₀O₂: *m/z* = 199.07 [M + H]⁺.

10. *2,4-Difluoro-1,1'-biphenyl* (Table 5, entry 10): Pale yellow crystals. Melting point = 61–63 °C; ¹H NMR (400 MHz, CDCl₃): δ (ppm) = 7.12–7.14 (m, 4H), 7.35–7.37 (m, 2H), 7.52 (d, *J* = 8.0 Hz, 2H). LC-MS for C₁₂H₈F₂: *m/z* = 191.03 [M+H]⁺.

11. *4-Hydroxybiphenyl* (Table 5, entries 11 and 15): White crystals. Melting point = 164–167 °C; ¹H NMR (400 MHz, CDCl₃): δ (ppm) = 4.91 (s, 1H), 6.82 (d, *J* = 8.0 Hz, 2H), 7.24 (m, 1H), 7.35 (d, *J* = 6.0 Hz, 2H), 7.41 (d, *J* = 8.0 Hz, 2H), 7.45 (d, *J* = 8.0 Hz, 2H). LC-MS for C₁₂H₁₀O: *m/z* = 171.09 [M+H]⁺.

12. *4-Phenylbenzophenone*: (Table 5, entry 12): Crystalline powder, Melting point = 102–105 °C; ¹H NMR (400 MHz, CDCl₃): δ (ppm) = 7.41–7.66 (m, 8H), 7.70–7.75 (m, 4H), 7.81 (d, *J* = 6.8 Hz, 2H), LC-MS for C₁₉H₁₄O: *m/z* = 259.23 [M+H]⁺.

13. *4-Methoxybiphenyl* (Table 5, entry 13): White powder. Melting point = 86–89 °C; ¹H NMR (400 MHz, CDCl₃): δ (ppm) = 3.84 (s, 3H), 6.97 (d, *J* = 8.0 Hz, 2H), 7.29 (t, *J* = 7.2 Hz, 1H), 7.41 (t, *J* = 7.6 Hz, 2H), 7.51–7.55 (m, 4H). LC-MS for C₁₃H₁₂O: *m/z* = 185.10 [M+H]⁺.

14. *4-(tert-butyl)-1,1'-biphenyl*: (Table 5, entry 14): Light brown powder, Melting point = 50–53 °C; ¹H NMR (400 MHz, CDCl₃): δ (ppm) = 1.35 (s, 9H), 7.41–7.47 (m, 5H), 7.66–7.68 (m, 2H), 7.82 (d, *J* = 8.4 Hz, 2H), LC-MS for C₁₆H₁₈: *m/z* = 211.05 [M+H]⁺.

15. *2-Methoxybiphenyl* (Table 5, entry 19): White powder. Melting point = 30–33 °C; ¹H NMR (400 MHz, CDCl₃): δ (ppm) = 3.75 (s, 3H), 6.91–6.98 (m, 2H), 7.24–7.27 (m, 3H), 7.34 (t, *J* = 7.8 Hz, 2H), 7.46 (d, *J* = 6.0 Hz, 2H). LC-MS for C₁₃H₁₂O: *m/z* = 185.23 [M+H]⁺.

2.3.6. General procedure for reduction of nitroarene reactions catalyzed by MNPs@SB-Pd nanomagnetic catalyst

In a round-bottomed flask equipped with nitroarene, MNPs@SB-Pd nanomagnetic catalyst (0.05 mol% Pd with respect to nitroarene), NaBH₄ (2.0 equiv) and H₂O (10 mL) were added and stirred under air atmosphere at room temperature for designated time. The progress of the reaction was monitored using TLC. After completion of the reaction, dichloromethane (20 mL) was added and the MNPs@SB-Pd nanomagnetic catalyst was separated using an external magnet. The organic layer was washed with water (3 × 10 mL) and dried over anhydrous

MgSO₄. The crude reduced product was isolated by column chromatography over silica gel using hexane and ethyl acetate to afford the corresponding pure reduced products in excellent yields. All the reduced products were known molecules and were confirmed by comparing the melting point, ¹H NMR and mass spectroscopic data with authentic samples.

1. *Phenylamine* (Table 8, entry1): Colorless liquid; ¹H NMR (400 MHz, CDCl₃): δ (ppm) = 3.54 (s, 2H), 6.68 (d, *J* = 8.8 Hz, 2H), 6.71 (t, *J* = 7.6 Hz, 1H), 7.18 (d, *J* = 8.8 Hz, 2H), LC-MS for C₆H₇N: *m/z* = 94.26 [M+H]⁺.

2. *4-Aminobenzoic acid* (Table 8, entry 2): Off-white solid, Melting point = 187-189 °C; ¹H NMR (400 MHz, CDCl₃): δ (ppm) = 5.91 (s, 2H), 7.52 (d, *J* = 7.2 Hz, 2H), 7.76 (d, *J* = 7.2 Hz, 2H), LC-MS for C₇H₇NO₂: *m/z* = 138.17 [M+H]⁺.

3. *3-Aminobenzaldehyde* (Table 8, entry 3): Pale yellow solid, Melting point = 29-32 °C; ¹H NMR (400 MHz, CDCl₃): δ (ppm) = 4.55 (s, 2H), 6.54 (d, *J* = 8.4 Hz, 1H), 6.66-6.69 (m, 2H), 7.47 (t, *J* = 7.6 Hz, 1H), 9.99 (s, 1H), LC-MS for C₇H₇NO: *m/z* = 122.13 [M+H]⁺.

4. *Benzene-1,3-diamine* (Table 8, entries 4 and 6): Colorless solid, Melting point = 64-67 °C; ¹H NMR (400 MHz, CDCl₃): δ (ppm) = 3.54 (s, 4H), 6.42-6.45 (m, 2H), 6.98 (s, 1H), 7.32 (t, *J* = 7.6 Hz, 1H), LC-MS for C₆H₈N₂: *m/z* = 109.19 [M+H]⁺.

5. *1-(4-aminophenyl)ethanone* (Table 8, entry 7): Pale yellow solid, Melting point = 104-108 °C; ¹H NMR (400 MHz, CDCl₃): δ (ppm) = 5.65 (s, 2H), 7.12 (d, *J* = 8.8 Hz, 2H), 7.54 (d, *J* = 8.4 Hz, 2H), 9.69 (s, 1H), LC-MS for C₈H₉NO: *m/z* = 136.18 [M+H]⁺.

6. *Benzene-1,4-diamine* (Table 8, entry 8): white solid, Melting point = 137-142 °C; ¹H NMR (400 MHz, CDCl₃): δ (ppm) = 3.58 (s, 4H), 6.83-6.85 (m, 4H), LC-MS for C₆H₈N₂: *m/z* = 109.15 [M+H]⁺.

7. *4-Aminobenzaldehyde* (Table 8, entry 9): Pale yellow solid, Melting point = 77-79 °C; ¹H NMR (400 MHz, CDCl₃): δ (ppm) = 5.65 (s, 2H), 7.14 (d, *J* = 8.8 Hz, 2H), 7.52 (d, *J* = 8.4 Hz, 2H), 9.67 (s, 1H), LC-MS for C₇H₇NO: *m/z* = 122.13 [M+H]⁺.

2.3.7. Procedure for recovery of MNPs@SB-Pd nanomagnetic catalyst

After completion of the reaction, MNPs@SB-Pd nanomagnetic catalyst was separated using a permanent magnet from the reaction mixture. The separated MNPs@SB-Pd nanomagnetic catalyst was then washed with water (2 x 10 mL) followed by ethanol (2 x 10 mL)

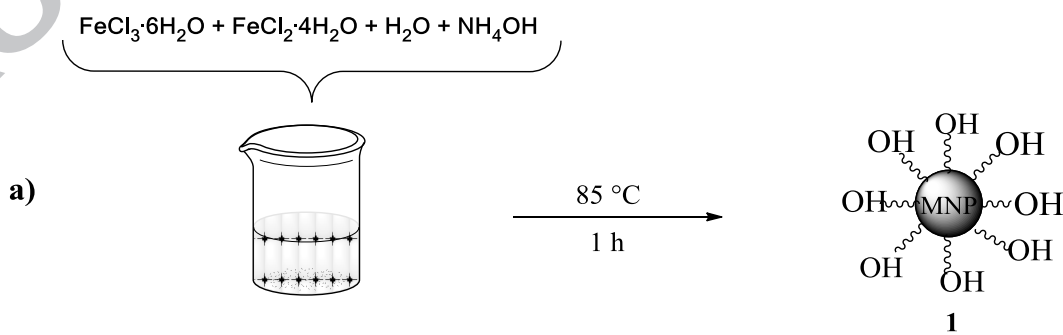
and dried at 45 °C for 12 h. Then, dried MNPs@SB-Pd nanomagnetic catalyst was used for next round of reaction without further purification.

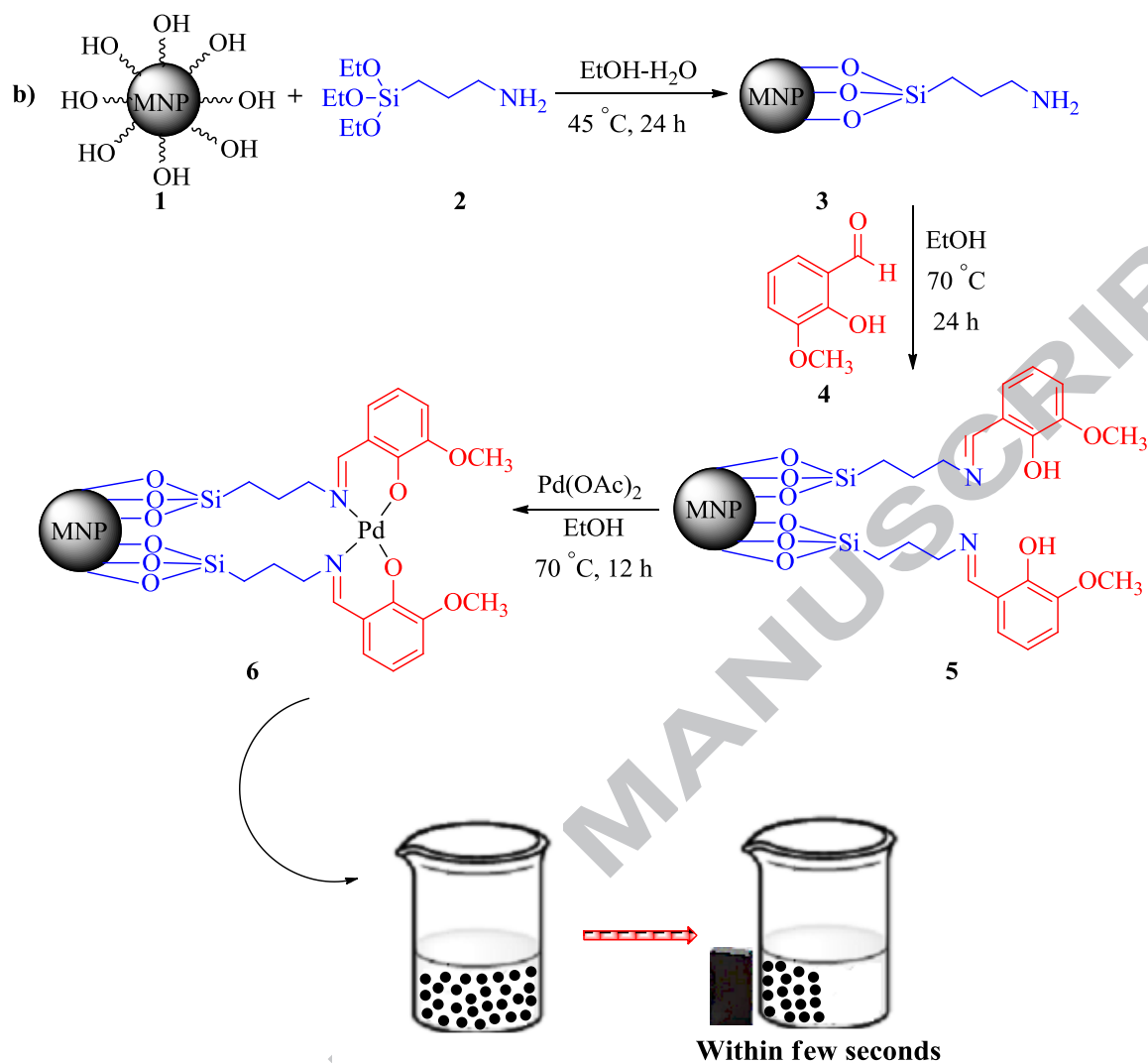
3. Results and Discussion

3.1. MNPs@SB-Pd nanomagnetic catalyst preparation

In continuation of our studies on the applications of magnetic nanoparticles tethered palladium(II) complexes in various organic reactions [39, 40], herein, we report a simple and efficient greener method for Suzuki-Miyaura cross-coupling between phenylboronic acid and a range of aryl halides containing iodo, bromo and chloro moieties and also for the reduction of nitroarenes in the presence of MNPs@SB-Pd nanomagnetic catalyst.

The MNPs@SB-Pd nanomagnetic catalyst was synthesized using a procedure shown in Scheme 1. Initially, hydroxyl substituted magnetic nanoparticles (**1**) were synthesized from chemical co-precipitation method using $\text{FeCl}_3 \cdot 6\text{H}_2\text{O}$ and $\text{FeCl}_2 \cdot 4\text{H}_2\text{O}$ in basic solution at 85 °C. Subsequently hydroxyl substituted magnetic nanoparticles were coated with (3-aminopropyl)triethoxysilane (**2**) to obtain the amine functionalized magnetic nanoparticles (**3**). Afterwards, the reaction of amino groups with 2-hydroxy-3-methoxybenzaldehyde (**4**) gave the corresponding magnetic nanoparticle tethered Schiff base (**5**). Finally, magnetic nanoparticle tethered Schiff base palladium(II) (**6**) was prepared through coordination of palladium(II) acetate with magnetic nanoparticle tethered Schiff base.





Scheme 1. Synthetic schemes of (a) hydroxyl substituted magnetic nanoparticles (MNPs) and (b) magnetic nanoparticles supported Schiff base palladium(II) nanomagnetic catalyst.

3.2. Spectroscopic and microscopic characterization of MNPs@SB-Pd nanomagnetic catalyst

The newly synthesized MNPs@SB-Pd nanomagnetic catalyst was characterized from attenuated total reflectance infrared spectroscopy, ultraviolet-visible spectroscopy, inductively coupled plasma-atomic emission spectroscopy, energy-dispersive X-ray spectroscopy, field-emission scanning electron microscopy, transmission electron microscopy, X-ray powder

diffraction, thermogravimetric analysis and Brunauer-Emmett-Teller surface area analysis to know the structure and composition.

3.2.1. ATR-IR spectroscopy

Successful functionalization of the MNPs can be determined from the ATR-IR spectroscopic technique. ATR-IR spectra of (a) MNPs, (b) AFMNPs, (c) SB@MNPs and (d) MNPs@SB-Pd nanomagnetic catalyst are shown in Fig. 1. The ATR-IR spectrum of MNPs (Fig. 1a) exhibits a strong band at 546 cm^{-1} assigned to Fe-O bond vibration and a broad band at 3396 cm^{-1} is attributed to the presence of OH groups on the surface of the MNPs. The bands observed around 1007 and 2904 cm^{-1} are ascribed to the Si-O and C-H stretching vibrations of the propyl group from (3-aminopropyl)triethoxysilane apart from a Fe-O stretching vibration at 567 cm^{-1} of AFMNPs (Fig. 1b), which confirms the functionalization of aminopropyltriethoxysilane on the surface of the MNPs [39, 40]. A new peak observed at 1633 cm^{-1} attributed to C=N stretching vibrations of SB@MNPs (Fig. 1c) apart from Si-O stretching vibrations at 1007 cm^{-1} which proves the formation of Schiff base on the surface of MNPs [41, 42]. The ATR-IR spectrum of MNPs@SB-Pd nanomagnetic catalyst reveals typical bands at 2928 , 1452 , 1014 and 556 cm^{-1} attributed to aliphatic C-H stretching, aromatic C=C stretching, Si-O stretching and Fe-O stretching vibrations (Fig. 1d) [39, 40]. The absorption due to (C=N) in MNPs@SB-Pd is observed at 1633 cm^{-1} and has shifted to lower wave number at 1616 cm^{-1} in MNPs@SB-Pd indicating coordination of SB@MNPs through imine nitrogen to palladium (Fig. 1d) [41, 42]. Fig 2b and 2c demonstrated the ATR-IR spectra of five times recycled MNPs@SB-Pd nanomagnetic catalyst from Suzuki-Miyaura cross-coupling reaction and ten time recycled MNPs@SB-Pd nanomagnetic catalyst from reduction of nitroarene respectively. Results show

that recycled MNPs@SB-Pd nanomagnetic catalyst from both the reactions is intact except some slight shift in the peak positions.

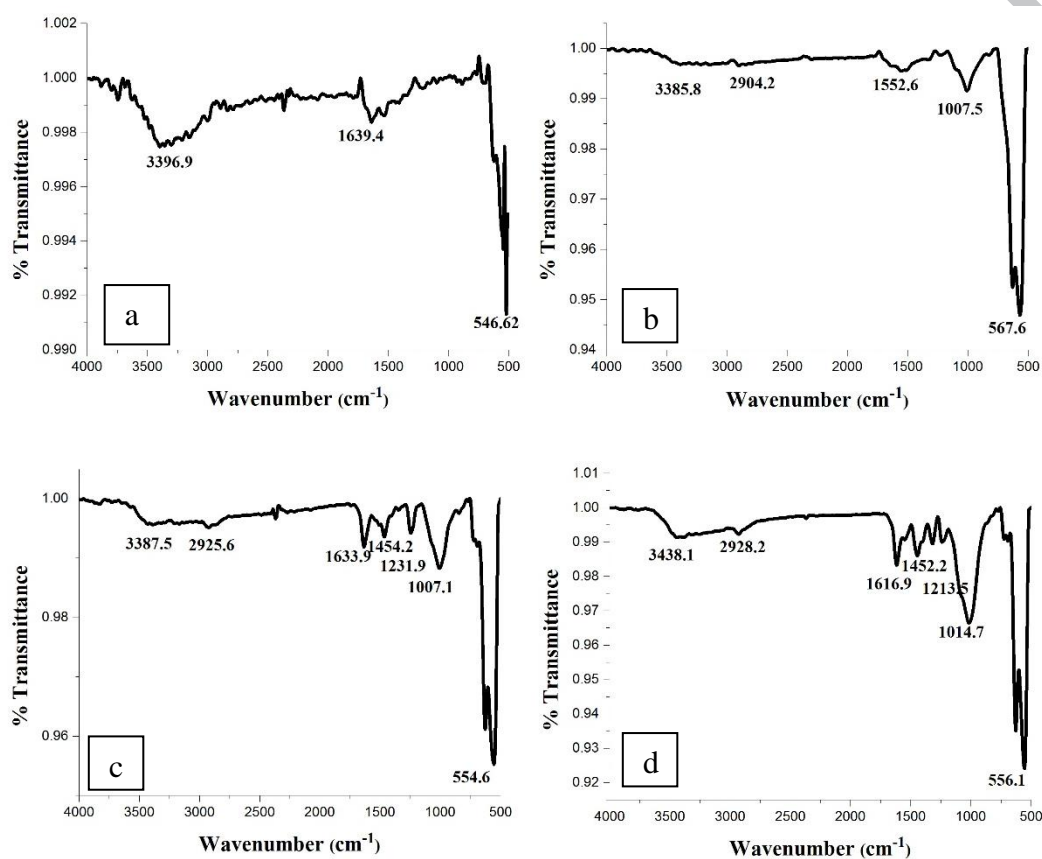


Fig. 1. ATR-IR spectra of (a) MNPs, (b) AFMNPs, (c) SB@MNPs and (d) MNPs@SB-Pd nanomagnetic catalyst.

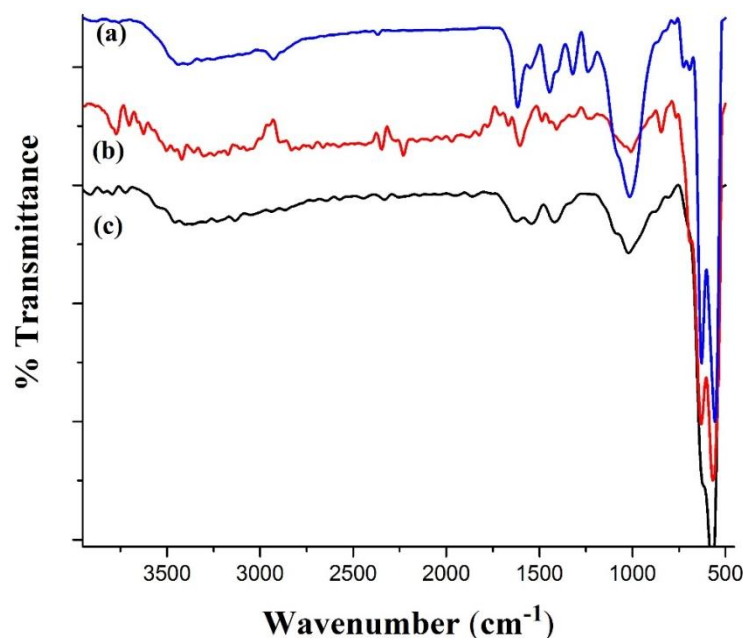


Fig. 2. ATR-IR spectra for (a) freshly prepared MNPs@SB-Pd nanomagnetic catalyst (b) Suzuki-Miyaura recycled MNPs@SB-Pd nanomagnetic catalyst and (c) reduction recycled MNPs@SB-Pd nanomagnetic catalyst.

3.2.2. UV-visible spectroscopy

The UV-visible spectra are often very helpful in the evaluation of results furnished by other methods of structural investigation. The UV-visible spectra of MNPs and MNPs@SB-Pd nanomagnetic catalyst were recorded at room temperature using water as the solvent (Fig. 3). The λ_{\max} observed for MNPs is 371 nm, whereas in the case of MNPs@SB-Pd nanomagnetic catalyst, the λ_{\max} observed is at 389 nm. The shift in λ_{\max} from 371 nm to 389 nm could be attributed to the successful surface functionalization of MNPs [43, 44].

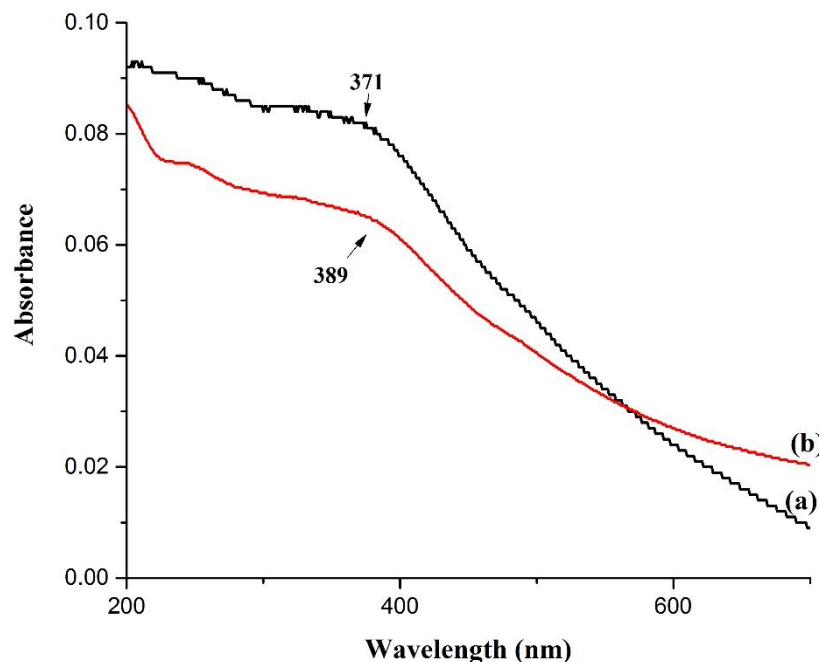


Fig. 3. UV-visible spectra of (a) MNPs and (b) MNPs@SB-Pd nanomagnetic catalyst.

3.2.3. Brunauer-Emmett-Teller surface area analysis

The surface functionalization of MNPs was additionally confirmed from analyzing the surface area by Brunauer-Emmett-Teller surface area analysis (BET). Nitrogen adsorption-desorption curves for (a) MNPs and (b) MNPs@SB-Pd nanomagnetic catalyst are shown in Fig. 4a and 4b. The MNPs@SB-Pd nanomagnetic catalyst exhibited a type-II isotherm. The amount of nitrogen adsorbed on the surface of MNPs is high compared to MNPs@SB-Pd. The surface area of bare MNPs is $77.48 \text{ m}^2\text{g}^{-1}$ which was reduced to $71.11 \text{ m}^2\text{g}^{-1}$ upon the formation of MNPs@SB-Pd nanomagnetic catalyst. The decrease in surface area reveals the successful functionalization of MNPs with Schiff base palladium(II) complex which is evident from data obtained from the BET [39, 40, 45].

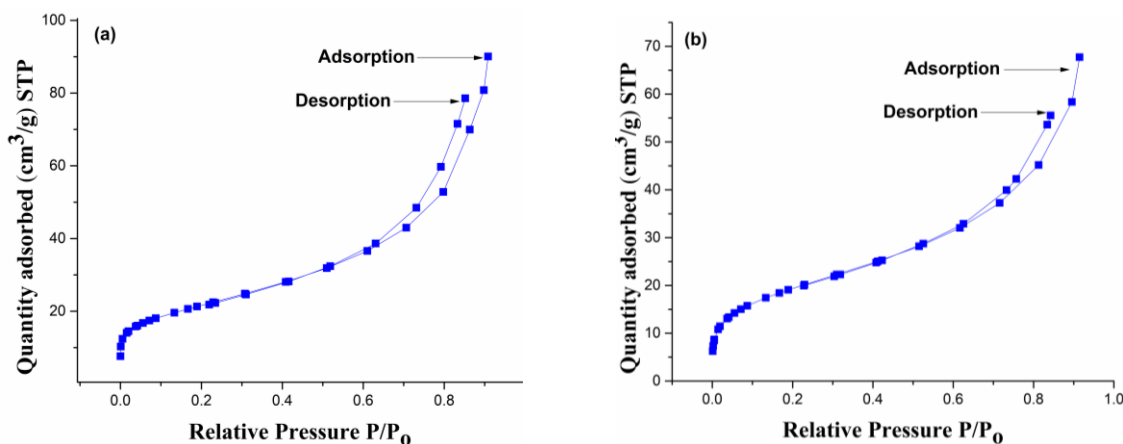


Fig. 4. Nitrogen adsorption-desorption curve for (a) MNPs and (b) MNPs@SB-Pd nanomagnetic catalyst.

3.2.4. Transmission electron microscopy (TEM)

The size and morphology of MNPs, fresh MNPs@SB-Pd nanomagnetic catalyst and five time recycled MNPs@SB-Pd nanomagnetic catalyst from Suzuki-Miyaura cross-coupling reaction were evaluated using transmission electron microscopy. The TEM images of (a) MNPs (b) MNPs@SB-Pd nanomagnetic catalyst and (c) five time recycled MNPs@SB-Pd nanomagnetic catalyst are shown in Fig. 5a, 5b and 5c. TEM image confirm the spherical shape of bare MNPs and size of the nanoparticles varied from 7 to 12 nm (Fig. 5a). On the other hand, TEM image of MNPs@SB-Pd nanomagnetic catalyst show that the nanoparticles are quite homogeneous and quasi-spherical with an average diameter of about 12-20 nm (Fig. 5d). In addition, the recycled MNPs@SB-Pd nanomagnetic catalyst did not show much change in morphology after being reused up to five times (Fig. 5c) [46-48].

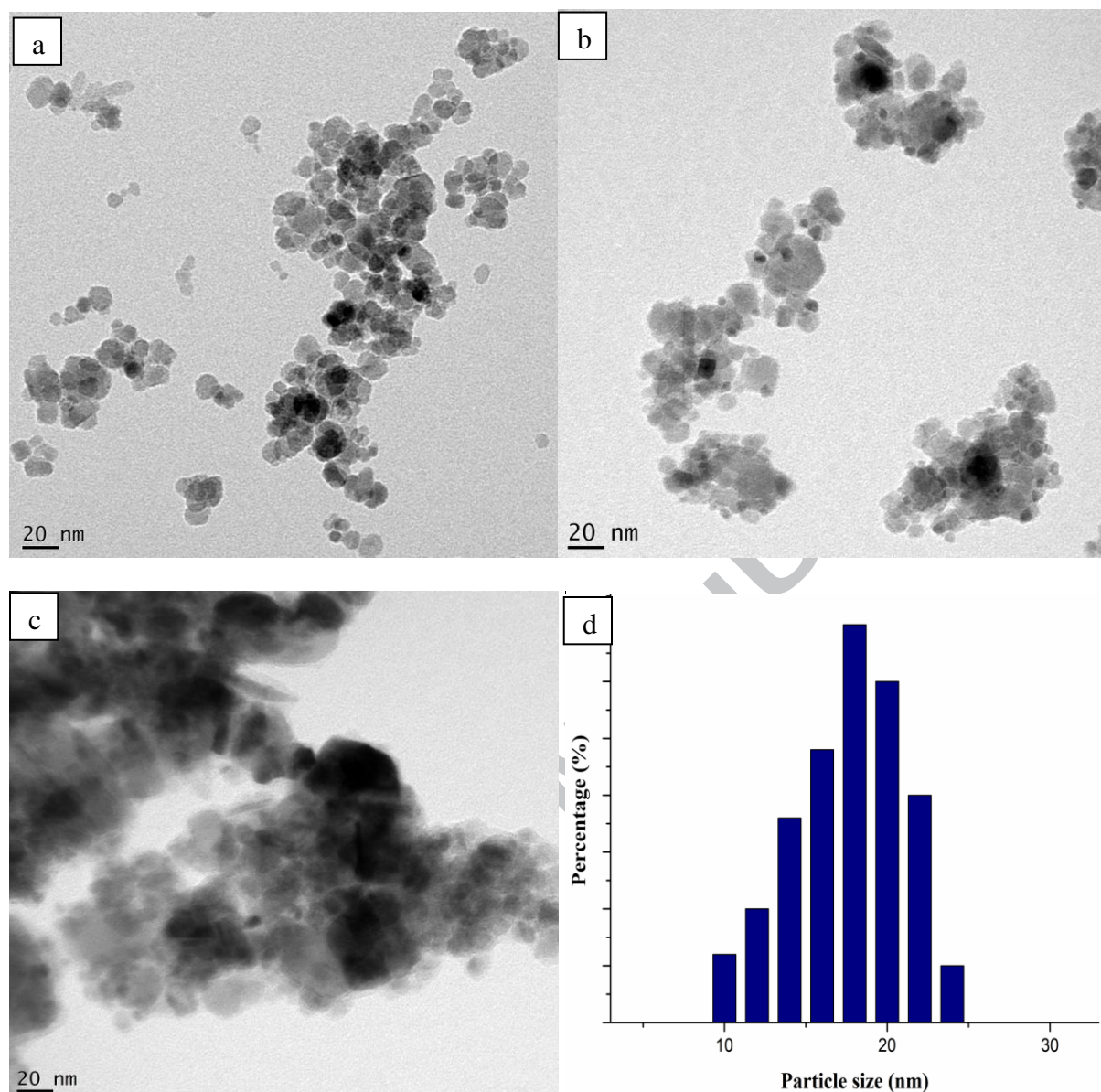


Fig. 5. TEM images of (a) MNPs, (b) MNPs@SB-Pd nanomagnetic catalyst, (c) five time recycled MNPs@SB-Pd nanomagnetic catalyst and (d) particle size distribution histogram.

3.2.5. Field emission scanning electron microscopy (FESEM)

In addition to the TEM image, in attempting to confirm the size and morphology of the freshly synthesized MNPs@SB-Pd nanomagnetic catalyst and five time recycled MNPs@SB-Pd nanomagnetic catalyst, SEM images were recorded and are shown in Fig. 6a and 6b. It can be inferred from the SEM images that the size of the freshly synthesized MNPs@SB-Pd

nanomagnetic catalyst particles is in the nanometer range in good accordance with the TEM image (Fig. 6a) [49-51]. After five recycles, the surface morphology of recycled MNPs@SB-Pd nanomagnetic catalyst remained almost same as that of freshly prepared MNPs@SB-Pd nanomagnetic catalyst as shown in Fig. 6b.

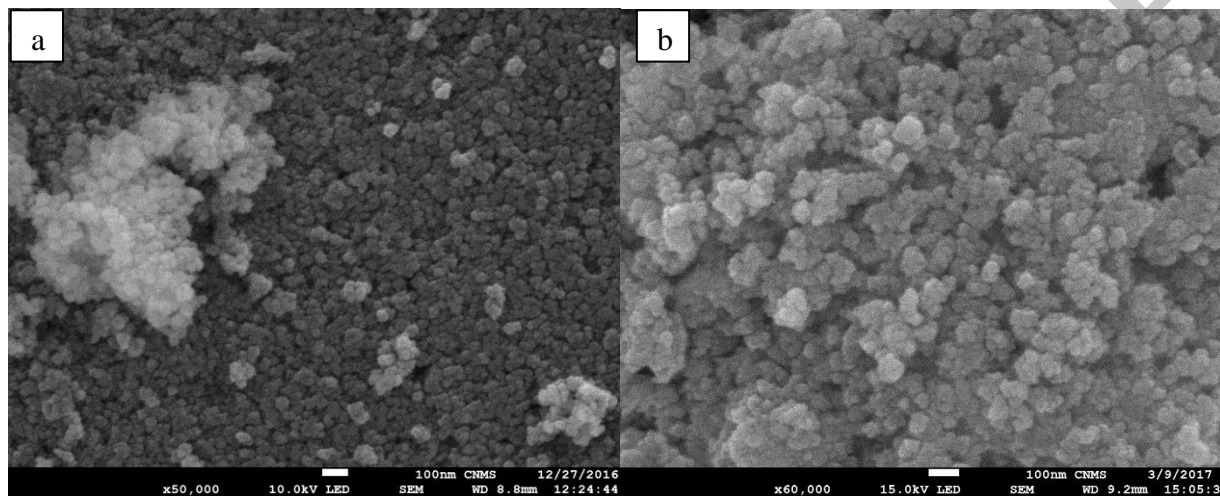
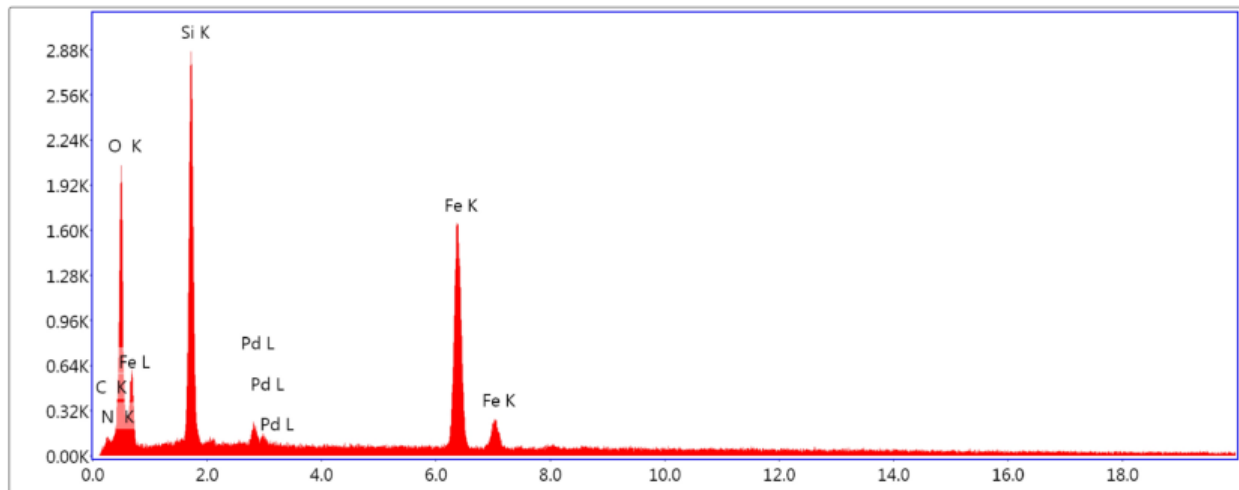


Fig. 6. FESEM images of (a) MNPs@SB-Pd nanomagnetic catalyst and (b) five time recycled MNPs@SB-Pd nanomagnetic catalyst.

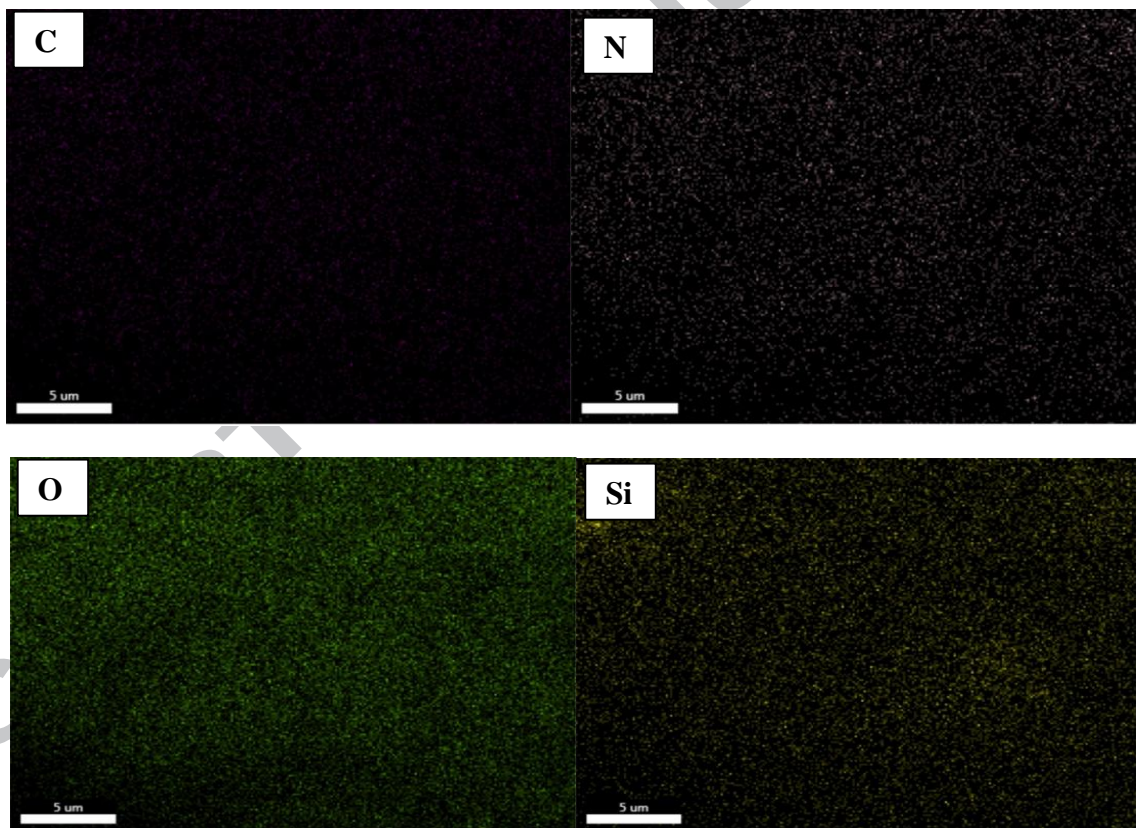
3.2.6. EDX analysis

Energy-dispersive X-ray spectroscopy is an analytical technique which is used for the elemental analysis of the newly synthesized MNPs@SB-Pd nanomagnetic catalyst. EDX spectra (Fig. 7) for MNPs@SB-Pd nanomagnetic catalyst shows different characteristic signals corresponding to C, N, O, Si, Fe and Pd atoms which validate the attachment of Schiff base-palladium(II) complex on the surface of MNPs [52]. Elemental mapping of MNPs@SB-Pd nanomagnetic catalyst was carried out to understand the distribution of elements in the MNPs@SB-Pd nanomagnetic catalyst as shown in Fig. 8. From elemental mapping data it is clear that all the elements are distributed evenly.



Lsec: 134.8 0 Cnts 0.000 keV Det: Element-C2 Det

Fig. 7. EDX spectrum of MNPs@SB-Pd nanomagnetic catalyst.



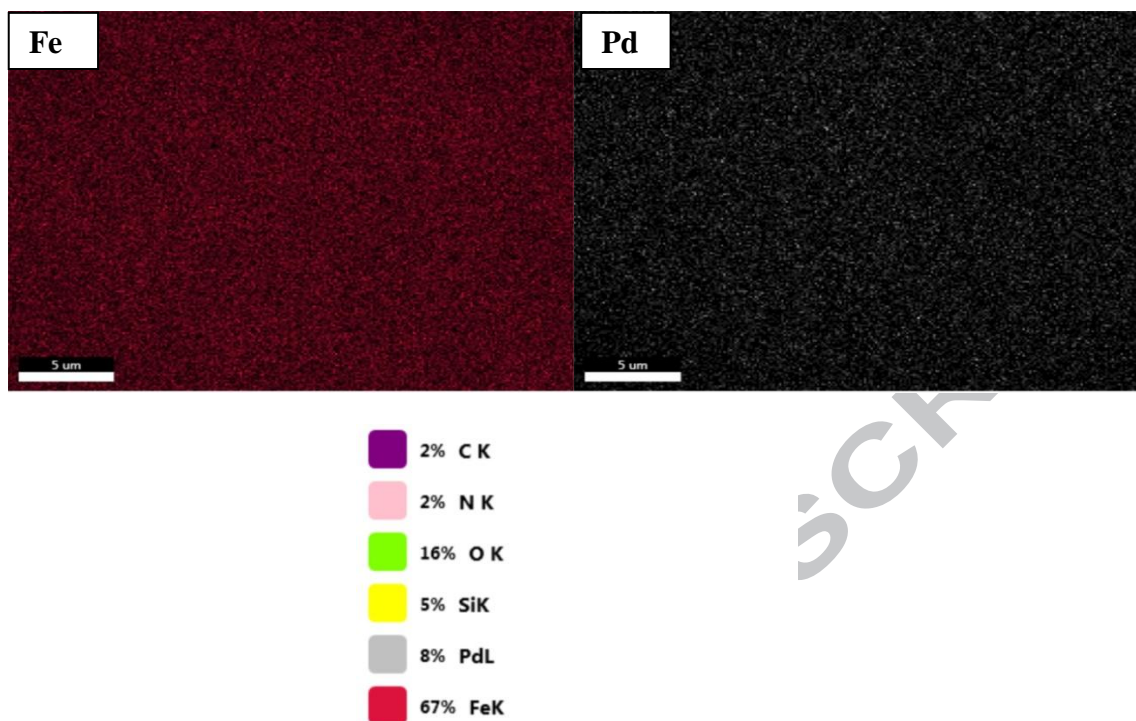


Fig. 8. Elemental mapping of MNPs@SB-Pd nanomagnetic catalyst.

3.2.7. ICP-AES analysis

Inductively coupled plasma atomic emission spectroscopy (ICP-AES) was employed to determine the exact quantity of palladium in the MNPs@SB-Pd nanomagnetic catalyst. From ICP-AES analysis, the amount of palladium loaded on the MNPs@SB-Pd nanomagnetic catalyst was found to be 5.43% w/w.

3.2.8. XRD analysis

The crystalline nature of the synthesized MNPs@SB-Pd nanomagnetic catalyst was established using XRD. The diffraction pattern for MNPs and MNPs@SB-Pd nanomagnetic catalyst is shown in Fig. 9a and 9b. XRD pattern of MNPs (Fig. 9a) reveals diffraction peaks at 2θ of 30.09° , 35.59° , 43.07° , 53.43° , 57.37° and 62.90° corresponding to the crystal planes of (220), (311), (400), (422), (511) and (440) which confirms cubic spinel structure of MNPs. Fig. 9b represents XRD pattern for MNPs@SB-Pd nanomagnetic catalyst which shows that the phase

remained unaltered even after the functionalization of MNPs which is in good agreement with the TEM image. Diffraction peaks at 2θ of 40.05° and 47.00° corresponding to the crystal planes of (111) and (200) shows the presence of palladium in the SB-Pd@MNPs nanomagnetic catalyst [53, 54].

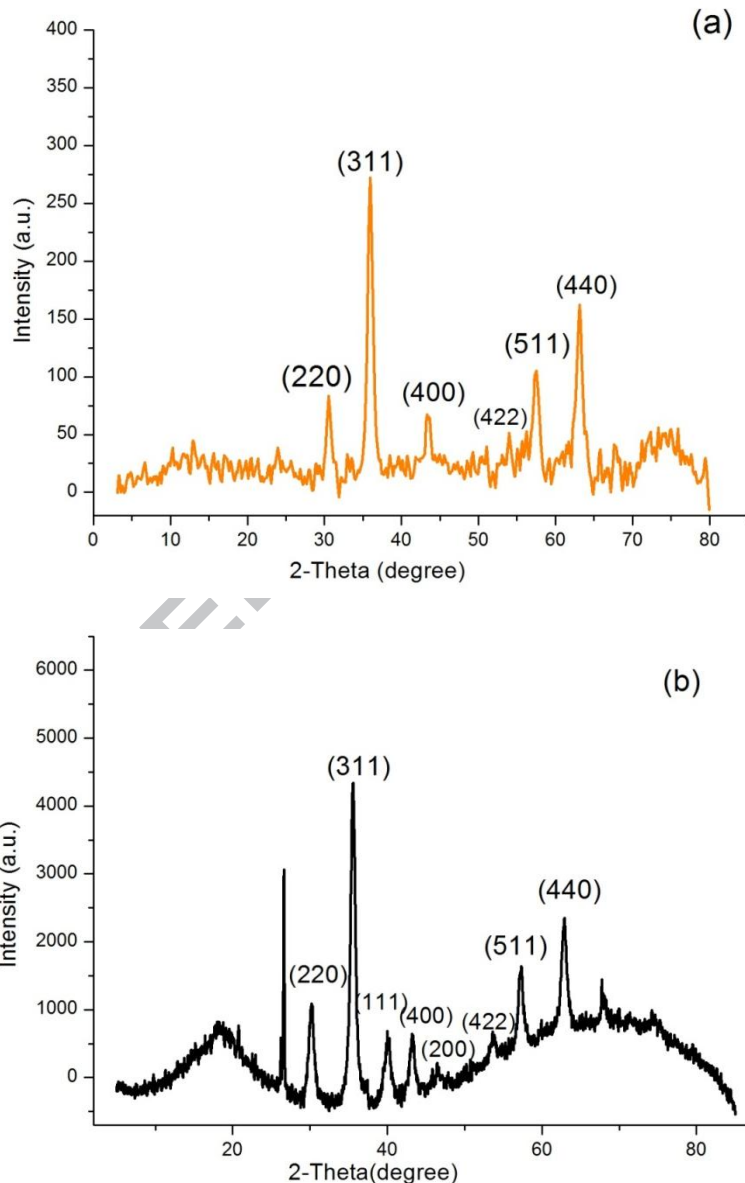


Fig. 9. XRD pattern of (a) MNPs and (b) MNPs@SB-Pd nanomagnetic catalyst.

3.2.9. Thermogravimetric analysis

The functionalization of MNPs with organic layer and Schiff base-palladium(II) complex is inferred using TGA. The thermal stability of MNPs and MNPs@SB-Pd nanomagnetic catalyst was determined through thermogravimetric analysis, which was carried out under an inert nitrogen atmosphere between 40 °C to 730 °C. Fig. 10a showed 4% weight loss in the range of 50-110 °C which is due to the loss of surface hydroxyl groups and moisture present on the surface of the magnetic nanoparticles. The MNPs@SB-Pd nanomagnetic catalyst (Fig.10b) decomposed in two steps. In first step, it showed the 1.5% weight loss in the range of 50°C to 110 °C correspond to the loss of physically adsorbed solvent and surface hydroxyl groups. In the second step, 6% mass loss in the range of 150-600 °C was observed which is due to the complete loss of covalently attached organic moiety. Therefore, from TGA result it is confirmed that the MNPs@SB-Pd nanomagnetic catalyst was successfully anchored on magnetic nanoparticles [49, 55]. Furthermore, on the basis of TGA results, it is clear that SB-Pd@MNPs nanomagnetic catalyst is stable up to a temperature of 200 °C which in turn allows the usage of this MNPs@SB-Pd nanomagnetic catalyst in reactions carried out at higher temperature up to 200 °C.

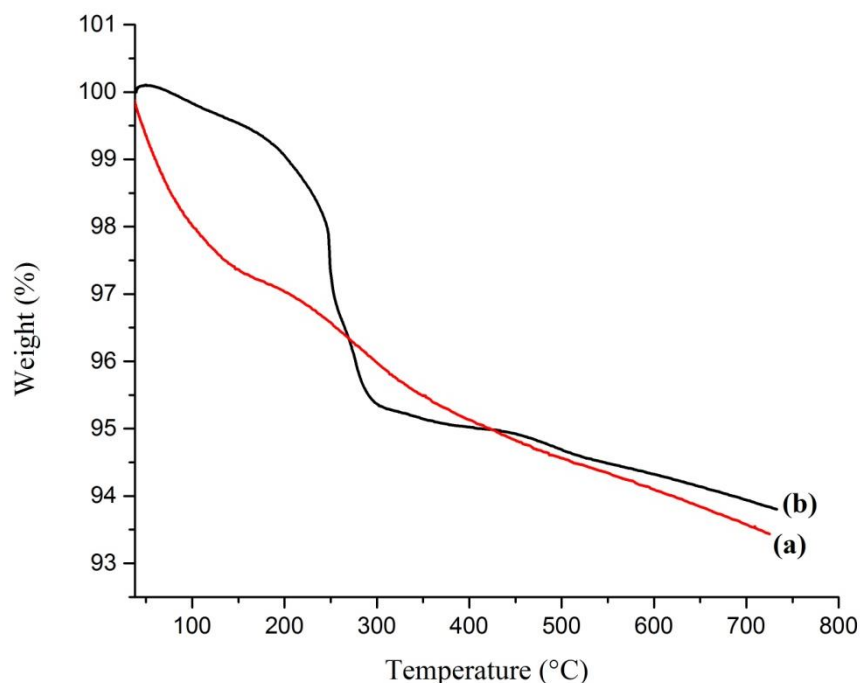


Fig. 10. TGA curves of (a) MNPs and (b) MNPs@SB-Pd nanomagnetic catalyst.

3.3. Catalytic activity of the MNPs@SB-Pd nanomagnetic catalyst in Suzuki-Miyaura cross-coupling reaction

MNPs@SB-Pd nanomagnetic catalyst was obtained as an air- and moisture stable catalyst. After structural characterization of the synthesized MNPs@SB-Pd nanomagnetic catalyst and in continuation of our work to test the catalytic potential and application of synthesized MNPs@SB-Pd nanomagnetic catalyst, we next investigated the catalytic effects of MNPs@SB-Pd nanomagnetic catalyst in Suzuki-Miyaura cross-coupling reaction. Initially, reaction conditions were optimized on model Suzuki-Miyaura cross-coupling reaction between 4-bromobenzonitrile and phenylboronic acid as shown in Scheme 2.



Scheme 2. Suzuki-Miyaura cross-coupling reaction between 4-bromobenzonitrile with phenylboronic acid in the presence of MNPs@SB-Pd nanomagnetic catalyst.

During the optimization of reaction conditions, environmentally benign solvents were given highest priority. Therefore, EtOH and H₂O were given highest priority as green solvent system. The reaction conditions were optimized with a series of Suzuki-Miyaura cross-coupling reactions of 4-bromobenzonitrile with phenylboronic acid in the presence of MNPs@SB-Pd nanomagnetic as shown in Table 1. The preliminary outcome revealed that using K₂CO₃ base, EtOH:H₂O (1:1) solvent mixture, 0.15 mol% Pd of MNPs@SB-Pd nanomagnetic catalyst at room temperature for 6 h resulted in highest yield (Table 1, entry 5). Then catalytic potential of MNPs@SB-Pd nanomagnetic catalyst for varying base, solvent, temperature, time and catalyst ratio were also studied for the model reaction.

Table 1

Optimization of conditions for Suzuki-Miyaura cross-coupling reaction of 4-bromobenzonitrile with phenylboronic acid in the presence of MNPs@SB-Pd nanomagnetic catalyst^a.

Entry	Base	Solvent	Temperature (°C)	Time (h)	Yield (%) ^b
1	K ₂ CO ₃	EtOH	RT	10	80
2	K ₂ CO ₃	MeOH	RT	18	74
3	K ₂ CO ₃	H ₂ O	RT	9	78
4	K ₂ CO ₃	EtOH:H ₂ O (2:1)	RT	7	85
5	K₂CO₃	EtOH:H₂O (1:1)	RT	6	87
6	K ₂ CO ₃	DMF	RT	5	59
7	NaOH	EtOH	RT	5	50
8	KOH	EtOH	RT	7	38
9	Na ₂ CO ₃	EtOH:H ₂ O (1:1)	RT	6	35
10	Na ₃ PO ₄ ·12H ₂ O	EtOH	RT	8	56
11	K ₂ CO ₃	MeOH	RT	18	74
12	K ₂ CO ₃	EtOH	RT	10	80
13	K ₂ CO ₃	H ₂ O	RT	9	78
14	K ₂ CO ₃	Acetone	RT	24	37
15	K ₂ CO ₃	DCM	RT	7	58
16	K ₂ CO ₃	CH ₃ CN	RT	5	-

17	K ₂ CO ₃	Toluene	RT	10	67
18	K ₂ CO ₃	DMF	RT	5	59
19	K ₂ CO ₃	THF	RT	24	-
20	K ₂ CO ₃	2-propanol	RT	26	31

^aReaction conditions: 4-bromobenzonitrile (1.0 mmol), phenylboronic acid (1.1 mmol), MNPs@SB-Pd(0.15 mol% palladium with respect to aryl halide), base (2.2 mmol) and solvent (10mL) in air. ^bIsolated yield after separation by column chromatography; average of two runs.

3.3.1. Effect of solvent on Suzuki-Miyaura cross-coupling reaction

The efficiency of various solvents such as EtOH, MeOH, H₂O, acetone, dichloromethane (DCM), acetonitrile (CH₃CN), toluene, dimethylformamide (DMF), tetrahydrofuran (THF), 2-propanol and EtOH:H₂O (1:1) solvent mixture were examined. From the results obtained, it is clear that the reaction proceeded smoothly with high yield in polar solvent like MeOH, EtOH, H₂O and EtOH:H₂O (1:1) solvent mixture (Table 1, entries 11-13 and 5). When DCM, toluene and DMF were used, cross-coupled product yield was medium (Table 1, entries 15, 17 and 18). In case of acetone and 2-propanol, the rate of reaction was slow and cross-coupled product yield was less (Table 1, entries 14 and 20). On the other hand, in CH₃CN and THF, reaction did not proceed (Table 1, entries 16 and 19). However, EtOH:H₂O (1:1) solvent mixture as a green solvent appears to be superior to the others (Table 1, entry 5).

Table 2

Suzuki-Miyaura cross-coupling reactions of 4-bromobenzonitrile with phenylboronic acid using MNPs@SB-Pd nanomagnetic catalyst with varying base and temperature^a.

Entry	Base	Solvent	Temperature(°C)	Time(h)	Yield (%) ^b
1	Na ₂ CO ₃	EtOH:H ₂ O (1:1)	RT	6	35
2	K₂CO₃	EtOH:H₂O (1:1)	RT	6	87
3	NaOH	EtOH:H ₂ O (1:1)	RT	5	50
4	KOH	EtOH:H ₂ O (1:1)	RT	7	38
5	Na ₃ PO ₄ ·12H ₂ O	EtOH:H ₂ O (1:1)	RT	8	56
6	KF	EtOH:H ₂ O (1:1)	RT	9	47

7	Cs ₂ CO ₃	EtOH:H ₂ O (1:1)	RT	9	55
8	NEt ₃	EtOH:H ₂ O (1:1)	RT	8	47
9	K ₂ CO ₃	EtOH:H ₂ O (1:1)	0	6	30
10	K ₂ CO ₃	EtOH:H ₂ O (1:1)	15	6	61
11	K ₂ CO ₃	EtOH:H ₂ O (1:1)	40	6	87
12	K ₂ CO ₃	EtOH:H ₂ O (1:1)	50	5	82
13	K ₂ CO ₃	EtOH:H ₂ O (1:1)	60	5	83
14	K ₂ CO ₃	EtOH:H ₂ O (1:1)	70	5	84

^aReaction conditions: 4-bromobenzonitrile (1.0 mmol), phenylboronic acid (1.1 mmol), MNPs@SB-Pd (0.15 mol% palladium with respect to aryl halide), base (2.2 mmol) and solvent (10 mL) in air. ^bIsolated yield after separation by column chromatography; average of two runs.

3.3.2. Effect of base on Suzuki-Miyaura cross-coupling reaction

The influence of various bases (Na₂CO₃, K₂CO₃, NaOH, KOH, Na₃PO₄·12H₂O, KF, Cs₂CO₃ and NEt₃) at room temperature using EtOH:H₂O (1:1) solvent system and MNPs@SB-Pd (0.15 mol% Pd with respect to aryl halide) nanomagnetic catalyst was studied in Suzuki-Miyaura cross-coupling reaction between 4-bromobenzonitrile and phenylboronic acid. Among these bases, Na₂CO₃, K₂CO₃, Na₃PO₄·12H₂O and Cs₂CO₃ were found to be rather effective (Table 2, entries 1, 2, 5 and 7) bases for Suzuki-Miyaura cross-coupling reaction. On the other hand, bases like NaOH, KOH, KF and NEt₃ showed lower conversion and lesser yields (Table 2, entries 3, 4, 6 and 8). As evident from Table 2, base K₂CO₃ gave the highest yield (Table 2, entry 2).

3.3.3. Effect of temperature on Suzuki-Miyaura cross-coupling reaction

To discover the catalytic potential of newly synthesized MNPs@SB-Pd nanomagnetic catalyst towards Suzuki-Miyaura cross-coupling reaction of 4-bromobenzonitrile with phenylboronic acid at varying temperatures, the model reaction was carried out at different temperatures as shown in Table 2. Results shown that at higher temperatures (40, 50, 60 and 70 °C) (Table 2, entries 11-14) the yields were almost same as that of room temperature (Table 2,

entry 2). However, at below room temperature (0 and 15 °C), the rate of catalytic activity was decreased with lower yields (Table 2, entries 9 and 10). Overall, the best yield of the cross-coupling reaction was observed at room temperature (Table 2, entry 2).

3.3.4. Effect of time on Suzuki-Miyaura cross-coupling reaction

To know the effect of time, Suzuki-Miyaura cross-coupling reaction of 4-bromobenzonitrile with phenylboronic acid was exposed at different time intervals with MNPs@SB-Pd nanomagnetic catalyst as summarized in Table 3. It is clear from the results obtained that the yield of the Suzuki-Miyaura cross-coupling reaction increased with increase in time (Table 3, entries 1-6) and further yield improvement was not observed after a time interval of 6 h (Table 3, entries 6 and 7). Hence, 6 h is the optimum time required for the maximum yield (Table 3, entry 6).

Table 3

Suzuki-Miyaura cross-coupling reactions of 4-bromobenzonitrile with phenylboronic acid using MNPs@SB-Pd nanomagnetic catalyst at various time intervals^a.

Entry	Base	Solvent	Temperature (°C)	Time (h)	Yield (%) ^b
1	K ₂ CO ₃	EtOH:H ₂ O (1:1)	RT	1	67
2	K ₂ CO ₃	EtOH:H ₂ O (1:1)	RT	2	75
3	K ₂ CO ₃	EtOH:H ₂ O (1:1)	RT	3	80
4	K ₂ CO ₃	EtOH:H ₂ O (1:1)	RT	4	82
5	K ₂ CO ₃	EtOH:H ₂ O (1:1)	RT	5	83
6	K₂CO₃	EtOH:H₂O (1:1)	RT	6	87
7	K ₂ CO ₃	EtOH:H ₂ O (1:1)	RT	7	87

^aReaction conditions: 4-bromobenzonitrile (1.0 mmol), phenylboronic acid (1.1 mmol), MNPs@SB-Pd (0.15 mol% palladium with respect to aryl halide), base (2.2 mmol) and solvent (5 mL) in air. ^bIsolated yield after separation by column chromatography; average of two runs.

3.3.5. Effect of catalyst ratio on Suzuki-Miyaura cross-coupling reaction

Catalyst ratio plays an important role in organic transformations. Suzuki-Miyaura cross-coupling reaction between 4-bromobenzonitrile and phenylboronic acid was carried out with varying palladium ratio starting from 0.025 mol% to 0.20 mol% (Table 4, entries 1-7). Increase in catalyst ratio resulted in increased yield up to 0.15 mol% of palladium (Table 4, entries 1-6) and further increase in the catalyst ratio does not increase the yield (Table 4, entry 7). Hence, 0.15 mol% of palladium is the best catalyst ratio required for the maximum yield (Table 4, entry 6) for Suzuki-Miyaura cross-coupling reaction between 4-bromobenzonitrile and phenylboronic acid.

Table 4

Suzuki-Miyaura cross-coupling reaction of 4-bromobenzonitrile with phenylboronic acid using different ratios of MNPs@SB-Pd nanomagnetic catalyst^a.

Entry	Base	Solvent	Temperature (°C)	Pd (mol%)	Yield (%) ^b
1	K ₂ CO ₃	EtOH:H ₂ O (1:1)	RT	0.025	35
2	K ₂ CO ₃	EtOH:H ₂ O (1:1)	RT	0.050	59
3	K ₂ CO ₃	EtOH:H ₂ O (1:1)	RT	0.075	63
4	K ₂ CO ₃	EtOH:H ₂ O (1:1)	RT	0.100	76
5	K ₂ CO ₃	EtOH:H ₂ O (1:1)	RT	0.125	82
6	K₂CO₃	EtOH:H₂O (1:1)	RT	0.15	87
7	K ₂ CO ₃	EtOH:H ₂ O (1:1)	RT	0.20	85

^aReaction conditions: 4-bromobenzonitrile (1.0 mmol), phenylboronic acid (1.1 mmol), base (2.2 mmol) and solvent (10 mL) in air. ^bIsolated yield after separation by column chromatography; average of two runs.

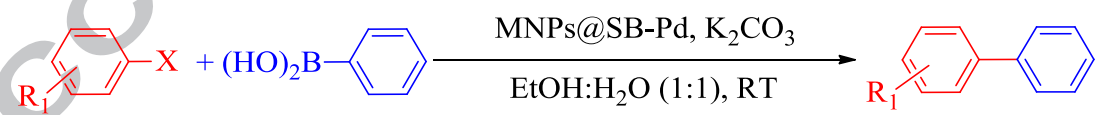
3.3.6. Suzuki-Miyaura cross-coupling reactions of different aryl halides

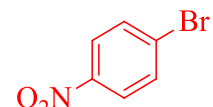
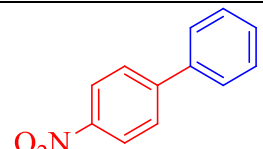
After optimization of the reaction conditions, the scope of MNPs@SB-Pd nanomagnetic catalyst was studied for Suzuki-Miyaura cross-coupling reaction of various aryl halides with phenylboronic acid and results are tabulated in Table 5. The experimental method is very simple

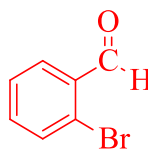
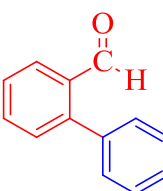
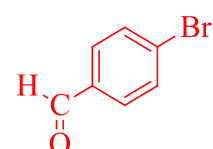
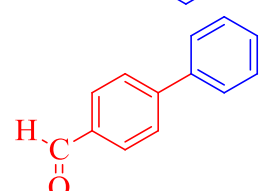
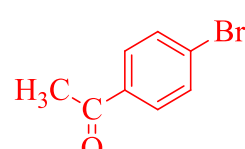
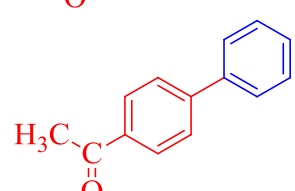
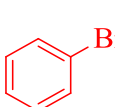
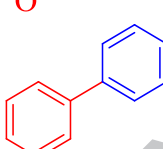
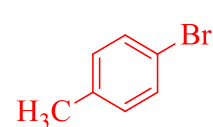
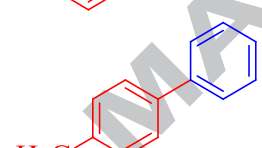
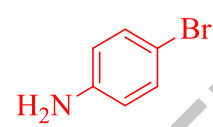
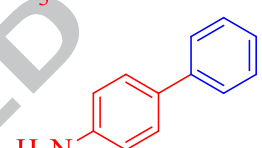
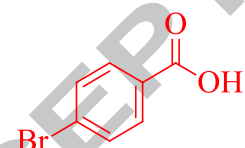
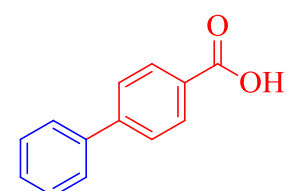
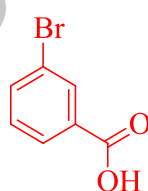
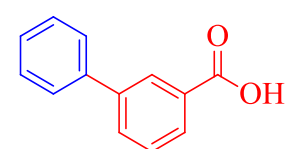
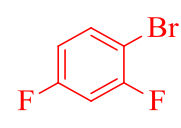
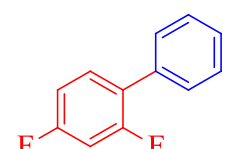
and convenient, and has the ability to tolerate a variety of functional groups. Aryl bromides with both electron withdrawing and electron donating substituents were exposed to Suzuki–Miyaura cross-coupling reaction using MNPs@SB-Pd nanomagnetic catalyst. The results show that all aryl bromides gave good to excellent yields irrespective of their electronic properties of the substituents by varying the reaction time but the steric effect played an important role in conversion of aryl bromide to product (Table 5, entries 1-14). Generally, aryl bromides and aryl iodide compounds except aryl chlorides reacted efficiently with phenylboronic acid giving cross-coupling products in good to excellent yield. However, reaction of aryl chlorides with phenylboronic acid gave cross-coupling products in low yield (Table 5, entries 15-18). On the other hand, selectivity of the MNPs@SB-Pd nanomagnetic catalyst was confirmed by the presence of a negligible amount of the homocoupled product obtained. For more clarification on selectivity, Suzuki–Miyaura cross-coupling reactions were carried out without aryl halides under optimized conditions. The biphenyl homocoupled product obtained was in trace amount, which concluded that the MNPs@SB-Pd nanomagnetic catalyst is highly selective.

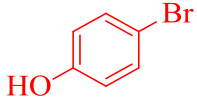
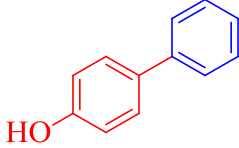
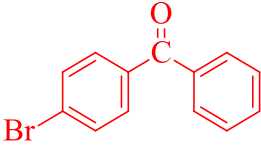
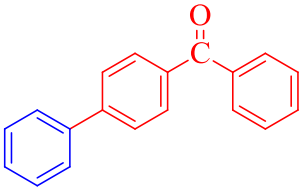
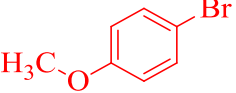
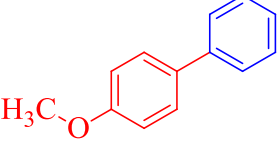
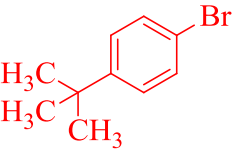
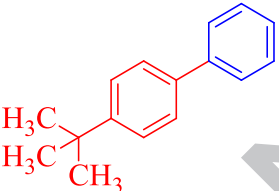
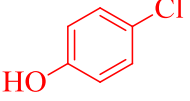
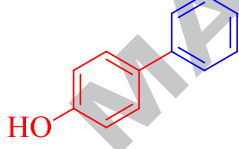
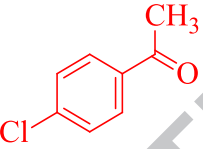
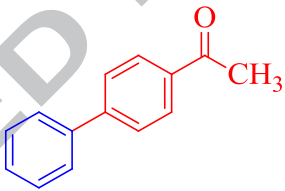

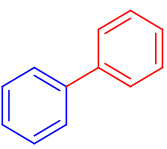
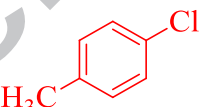
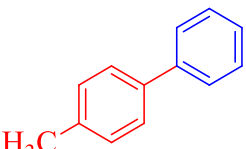
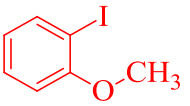
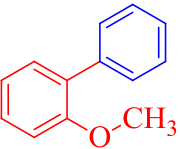
Table 5

Suzuki-Miyaura cross-coupling reactions between aryl halides with phenylboronic acid catalyzed by MNPs@SB-Pd nanomagnetic catalyst^a.



Entry	Aryl halides	Product	Time (h)	Yield (%) ^b	TON
1			5	88	144

2			7	65	117
3			15	69	124
4			23	88	146
5			3	69	147
6			2	73	143
7			6	84	162
8			5	76	128
9			14	69	114
10			14	65	112

11			5	91	176
12			12	61	77
13			2	70	127
14			12	65	101
15			12	55	141
16			15	60	129
17			13	37	108
18			12	57	151
19			2	80	116

^aReaction conditions: aryl halide (1.0 mmol), phenylboronic acid (1.1 mmol), MNPs@SB-Pd nanomagnetic catalyst (0.15 mol% Pd with respect to aryl halide), base (2.2 mmol) and EtOH:H₂O (10 mL) in air. ^bIsolated yield after separation by column chromatography; average of two runs.

3.3.7. Catalyst recyclability and leaching studies in Suzuki-Miyaura cross-coupling reaction

Recyclability is an important factor that judges the versatility and importance of the catalyst. Therefore, recyclability of MNPs@SB-Pd nanomagnetic catalyst was examined in the Suzuki-Miyaura cross-coupling reaction between 4-bromobenzonitrile and phenylboronic acid. After completion of each cycle, the MNPs@SB-Pd nanomagnetic catalyst can be efficiently recovered from the reaction mixture by using an external magnet, washed with ethanol and water and dried. The recovered MNPs@SB-Pd nanomagnetic catalyst can be reused up to five cycles without loss of catalytic activity and the results are shown in Fig. 11. Decrease in catalytic activity of MNPs@SB-Pd nanomagnetic catalyst was observed after five recycles towards Suzuki-Miyaura cross-coupling reaction. Five time recycled MNPs@SB-Pd nanomagnetic catalyst was characterized by ATR-IR, TEM and FESEM techniques. ATR-IR spectrum (Fig. 2b) shows that the MNPs@SB-Pd nanomagnetic catalyst is intact after recycling. Moreover, no change in the morphology was observed through the TEM image (Fig. 5c) of the MNPs@SB-Pd nanomagnetic catalyst after recycling up to five cycles, which is further confirmed by the FESEM image (Fig. 6b).

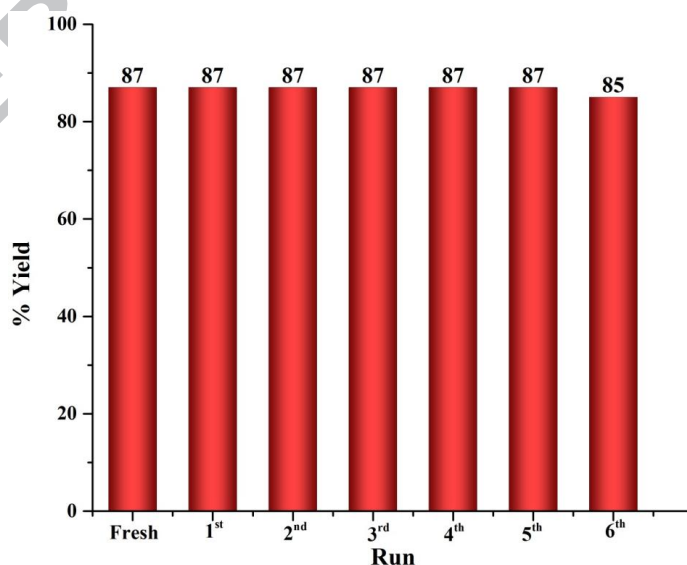


Fig. 11. The recycling efficiency of MNPs@SB-Pd nanomagnetic catalyst in Suzuki–Miyaura cross-coupling reaction of 4-bromobenzonitrile and phenylboronic acid

Leaching of palladium ion is a serious problem for supported palladium catalysts, and prevents catalyst separation and recycling. Therefore, leaching study was accomplished from the magnetic separation of the MNPs@SB-Pd nanomagnetic catalyst after 30 minutes of reaction time, and the same reaction was further continued for more than 6 h and the isolated yield was around 60%. This confers that leaching of palladium from the MNPs@SB-Pd nanomagnetic catalyst was not occurring possibly because of the specific nature of the designed MNPs@SB-Pd nanomagnetic catalyst.

3.3.8. Comparison of catalysts

In order to understand the uniqueness of the synthesized MNPs@SB-Pd nanomagnetic catalyst, we compared the results of Suzuki–Miyaura cross-coupling reactions of the MNPs@SB-Pd nanomagnetic catalyst with other supported heterogeneous catalysts, which is given in Table 6. Comparison of the results shows a better catalytic activity in shorter reaction time and milder reaction conditions for MNPs@SB-Pd nanomagnetic catalyst in the Suzuki–Miyaura cross-coupling reaction [52, 56-63].

Table 6

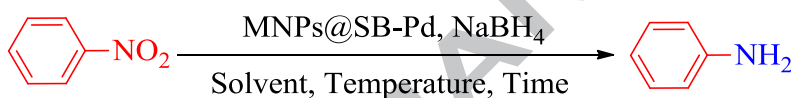
Comparison of results for the MNPs@SB-Pd nanomagnetic catalyst with other catalysts for the Suzuki–Miyaura cross-coupling reaction between 4-bromobenzonitrile and phenylboronic acid.

Entry	Catalyst	Solvent	Temp. (°C)	Time (h)	Yield (%)	Ref.
1	CL-Sc-Pd	Solvent free	50	0.1	80	[56]
2 ^a	M(P1)41	20% H ₂ O/EtOH	60	2.3	74	[57]
3	SMNPs-Salen Pd	DMF/H ₂ O	100	3	99	[58]
4	γ-Fe ₂ O ₃ -acetamidine-Pd	DMF	100	2	92	[59]

5	Cat-3	H ₂ O	80	12	99	[60]
6	Fe ₃ O ₄ /P(GMA-AA-MMA)-Schiff base-Pd	DMF/H ₂ O (1:1)	80	1	97	[61]
7	Pd Cat	EtOH/H ₂ O (1:1)	50	1	94	[62]
8	Pd(II)-NiFe ₂ O ₄	EtOH/H ₂ O (9:1)	80	4	92	[52]
9	Oxime-Palladacycle catalyst	EtOH/H ₂ O (1:1)	R.T	2	97	[63]
10	MNPs@SB-Pd	EtOH/H ₂ O (1:1)	R.T	6	87	[This work]
11 ^a	MNPs@SB-Pd	EtOH/H ₂ O (1:1)	R.T	23	88	[This work]

^aSuzuki–Miyaura cross-coupling reaction between 4-bromoacetophenone and phenylboronic acid.

3.4. Catalytic activity of the MNPs@SB-Pd nanomagnetic catalyst in reduction of nitroarenes



Scheme 3. Catalytic activity of the MNPs@SB-Pd nanomagnetic catalyst in the reduction of nitrobenzene.

The application of MNPs@SB-Pd nanomagnetic catalyst was also studied in the reduction of nitroarenes. In order to optimize the reaction conditions, reduction of nitrobenzene to aniline was used as model reaction (Scheme 3). During optimization of reaction conditions, various factors like mole ratio of NaBH₄, mole percentage of MNPs@SB-Pd nanomagnetic catalyst, and temperature were studied. As predicted, target product could not be detected in the absence of MNPs@SB-Pd nanomagnetic catalyst. The best results were achieved by carrying out the reaction with 2.0 equivalents of NaBH₄, H₂O as solvent (10 mL) and 0.05 mol% palladium of MNPs@SB-Pd nanomagnetic catalyst at room temperature in 2 minutes (Table 7, entry 5). The results are summarized in Table 7.

Table 7

Optimization of reaction conditions for nitrobenzene reduction with sodium borohydride in the presence of MNPs@SB-Pd nanomagnetic catalyst^a.

Entry	Solvents	NaBH ₄ (moles)	Pd (mol%)	Temperature (°C)	Time (h)	Yield (%) ^b
1	H ₂ O	3	-	RT	5.00	-
2	H ₂ O	3	0.02	RT	0.5	68
3	H₂O	2	0.05	RT	0.03	90
4	H ₂ O	3	0.05	RT	0.33	90
5	H ₂ O	3	0.07	RT	0.25	90
6	H ₂ O	1	0.05	RT	4.5	65
7	H ₂ O	1.5	0.05	RT	4.5	73

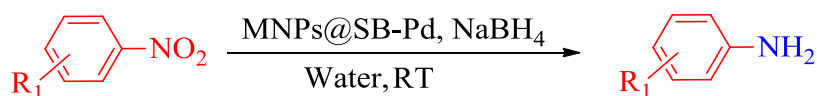
^aReaction conditions: nitrobenzene (1.0 mmol), and solvent (10 mL). ^bIsolated yield after separation by column chromatography; average of two runs.

3.4.1. Reduction of different nitroarenes

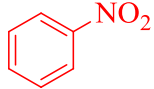
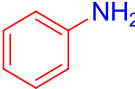
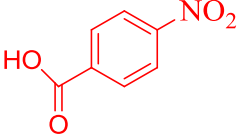
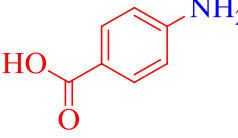
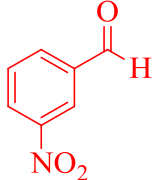
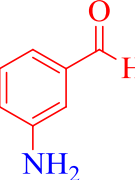
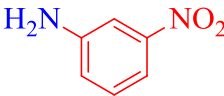
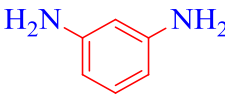
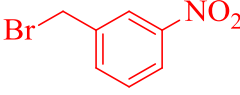
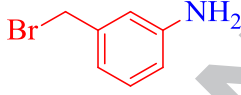
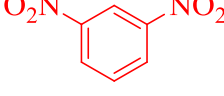
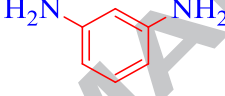
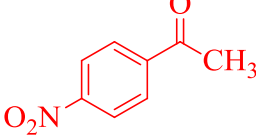
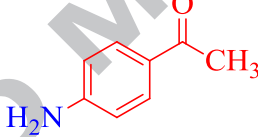
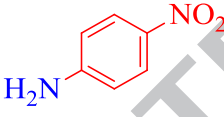
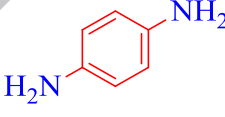
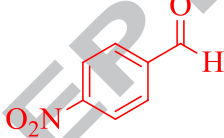
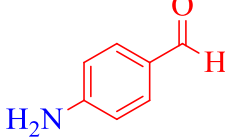
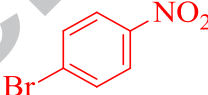
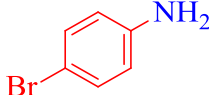
Under the optimized reaction conditions, wide ranges of substituted aromatic nitro compounds were reduced by this procedure to produce the corresponding aromatic amines. The results are summarized in Table 8. The reduction was almost uniform irrespective of the nature of substituent on the aromatic ring (Table 8, entries 1-10). Therefore, it is evident that our method is reasonably excellent and can be applied to several types of nitroarenes. Reduction of nitrobenzene to aniline shows less conversion in 2 minutes (Table 8, entry 1). We have also screened bromo nitroarenes but observed trace yields of desired products (Table 8, entries 5 and 10). Overall, the reductions are very clean, giving the amines in high yields. These all results confirmed that the newly synthesised MNPs@SB-Pd nanomagnetic catalyst could act as an excellent catalyst in reduction of nitroarenes.

Table 8

Nitroarenes reduction catalyzed by MNPs@SB-Pd nanomagnetic catalyst^a.



Entry	Nitroarenes	Product	Time (h)	Yield	TON
-------	-------------	---------	----------	-------	-----

				(%) ^b	
1			0.03	90	7302
2			0.16	88	5250
3			0.03	78	5118
4			0.08	85	6103
5			10.0	Trace	-
6 ^c			10	86	5178
7			3	90	5475
8			0.16	93	6658
9			0.16	83	5448
10			10.0	Trace	-

^aReaction conditions: nitroarene (1.0 mmol), NaBH₄ (2.0 mmol), MNPs@SB-Pd nanomagnetic catalyst(0.05 mol% palladium with respect to nitro compound) and water (10 mL). ^bIsolated yield after separation by column chromatography; average of two runs. ^c used 4.0 mmol NaBH₄

3.4.2. Catalyst recyclability in nitroarenes reduction

Recyclability is an important factor, which can judge the sustainability of a catalyst.

Hence, the recyclability of MNPs@SB-Pd was examined through reduction of nitrobenzene to

aniline with sodium borohydride. Synthesized MNPs@SB-Pd nanomagnetic catalyst was effectively recovered through applying an external magnetic field, washed with ethanol and water and dried. Then, recovered MNPs@SB-Pd nanomagnetic catalyst was reused for reduction of nitrobenzene to aniline under the optimized conditions and it was observed that there was no change in catalytic activity up to 10 recycles in the reduction of nitrobenzene with sodium borohydride and the results are shown in Fig. 12. Additionally, ATR-IR spectrum of ten times recycled MNPs@SB-Pd nanomagnetic catalyst was recorded and the spectrum (Fig. 2c) shows slight shift in the peaks from that of the fresh MNPs@SB-Pd nanomagnetic catalyst.

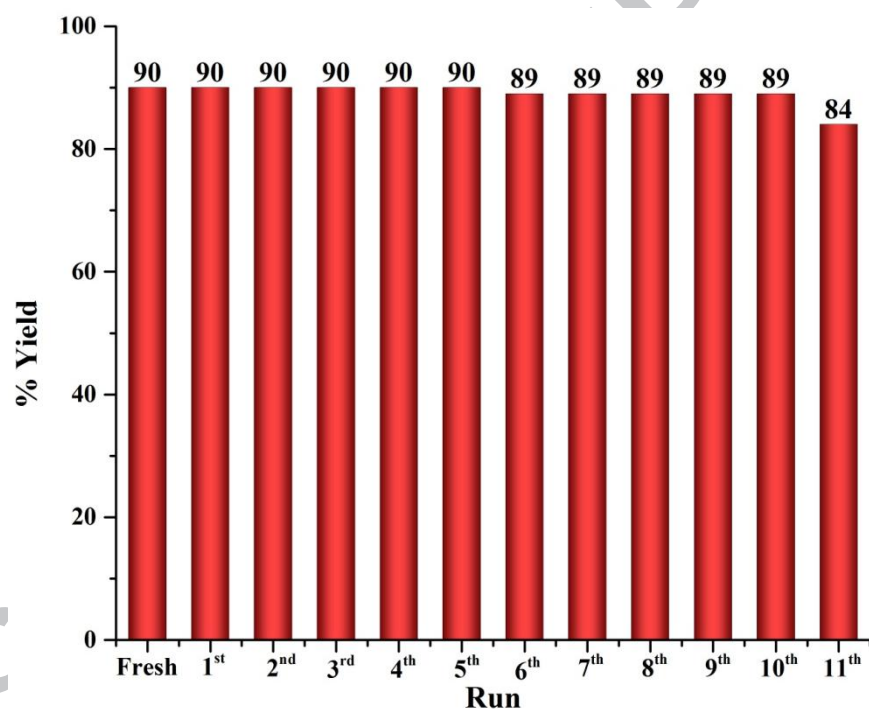


Fig. 12. The recycling efficiency of MNPs@SB-Pd nanomagnetic catalyst in nitroarene reduction reaction.

3.4.3. Comparison of catalysts

In order to show the effectiveness of the newly synthesized MNPs@SB-Pd nanomagnetic catalyst, the results obtained for the reduction of nitroarenes are compared with previously

reported catalysts. Comparison of the results displays enhanced catalytic activity in less time under mild reaction conditions for MNPs@SB-Pd nanomagnetic catalyst in reduction of nitroarenes (Table 9) [64-69].

Table 9

Comparison of results for the MNPs@SB-Pd nanomagnetic catalyst with other catalysts in nitrobenzene reduction reaction.

Entry	Catalyst	Solvent	Temp. (°C)	Time (h)	Yield (%)	Ref.
1	Cu-Acac@AM-Si-Fe ₃ O ₄	H ₂ O	R.T	0.2	97	[64]
2	[Pd(C ₆ H ₄ CH=N-P)(PhCN)Cl]	DMF	40	2.5	99	[65]
3	Pd(II)-Schiff base complex	DMF	R.T	2.8	98	[66]
4	[Pd ₂ (bnpn)(μ-OH)(CF ₃ COO) ₂] ⁺	Methanol	50	12	96	[67]
5	Pd/C	2-CH ₃ THF	R.T	3	85	[68]
6	Pd@CQD@Fe ₃ O ₄	H ₂ O:EtOH (5:1)	R.T	2	97	[69]
7	MNPs@SB-Pd	H ₂ O	R.T	0.03	90	[This work]

4. Conclusions

In this work, Schiff-base palladium(II) complex immobilized on magnetic nanoparticles was synthesized and characterized through ATR-IR, UV-Visible, ICP-AES, EDS, FESEM, TEM, XRD, TGA and BET analysis. The air- and moisture stable MNPs@SB-Pd nanomagnetic catalyst was used as an efficient catalyst for C-C bond formation through Suzuki-Miyaura cross-coupling reactions between phenylboronic acid and a range of aryl halides containing iodo, bromo and chloro moieties and reduction of nitroarenes. This MNPs@SB-Pd nanomagnetic catalyst shows notable advantages including simplicity of operation, excellent yields, short

reaction times and heterogeneous nature. More importantly, the MNPs@SB-Pd nanomagnetic catalyst could be easily recovered by external magnetic field and reused without any noticeable loss of activity at least five times in Suzuki–Miyaura cross-coupling and ten times in reduction of nitroarene reactions. In conclusion, it is intended that this study will open a gateway for the development of more sustainable catalytic processes.

Acknowledgements

The authors thank DST-Nanomission, India (SR/NM/NS-20/2014), DST-SERB, India (SERB/F/7013/2015-16) and Jain University, India for financial support.

References

- [1] A. Balanta, C. Godard, C. Claver, *Chem Soc Rev*, 40 (2011) 4973-4985.
- [2] N. Kambe, T. Iwasaki, J. Terao, *Chem Soc Rev*, 40 (2011) 4937-4947.
- [3] L. Yin, J. Liebscher, *Chem Rev*, 107 (2007) 133-173.
- [4] V. Resch, J.H. Schrittwieser, E. Siirola, W. Kroutil, *Curr Opin Biotechnol*, 22 (2011) 793-799.
- [5] M.E. Matheron, M. Porchas, *Plant Dis*, 88 (2004) 665-668.
- [6] J.K. Belardi, G.C. Micalizio, *Angew Chem Int Ed*, 47 (2008) 4005-4008.
- [7] Y. Jia, M. Bois-Choussy, J. Zhu, *Angew Chem Int Ed*, 47 (2008) 4167-4172.
- [8] J.A. Burlison, L. Neckers, A.B. Smith, A. Maxwell, B.S.J. Blagg, *J Am Chem Soc*, 128 (2006) 15529-15536.
- [9] W.A. Herrmann, *Angew Chem Int Ed*, 41 (2002) 1290-1309.
- [10] L. Botella, C. Nájera, *Angew Chem Int Ed*, 41 (2002) 179-181.
- [11] G.A. Grasa, A.C. Hillier, S.P. Nolan, *Org Lett*, 3 (2001) 1077-1080.
- [12] D.W. Old, J.P. Wolfe, S.L. Buchwald, *J Am Chem Soc*, 120 (1998) 9722-9723.

- [13] E. Morita, E.J. Young, *Rubber Chem Technol*, 36 (1963) 844-862.
- [14] N. Ono, Wiley VCH, DOI (2001) 30-69.
- [15] J.M. Buist, (1978) *Developments in polyurethanes*. Elsevier Science Ltd Vol 1.
- [16] F. Korte, (1975) *Methodicum Chemicum*. Vol 5, George Thieme, Stuttgart, pp 91-95.
- [17] K. Junge, K. Schroder, M. Beller, *Chem Commun* 47 (2011) 4849-4859.
- [18] C. Linares, M. Mediavilla, A.J. Pardey, P. Baricelli, C. Longo-Pardey, S.A. Moya, *Catal Lett*, 50 (1998) 183-185.
- [19] M. Orlandi, F. Tosi, M. Bonsignore, M. Benaglia, *Org Lett*, 17 (2015) 3941-3943.
- [20] C. Yu, B. Liu, L. Hu, *J Org Chem*, 66 (2001) 919-924.
- [21] S.A. Patil, C.-M. Weng, P.-C. Huang, F.-E. Hong, *Tetrahedron*, 65 (2009) 2889-2897.
- [22] Y.-C. Lai, H.-Y. Chen, W.-C. Hung, C.-C. Lin, F.-E. Hong, *Tetrahedron*, 61 (2005) 9484-9489.
- [23] A.K. Diallo, C. Ornelas, L. Salmon, J. Ruiz Aranzaes, D. Astruc, *Angew Chem Int Ed*, 46 (2007) 8644-8648.
- [24] J. Yang, D. Wang, W. Liu, X. Zhang, F. Bian, W. Yu, *Green Chem*, 15 (2013) 3429-3437.
- [25] E. Tyrrell, L. Whiteman, N. Williams, *J Organomet Chem*, 696 (2011) 3465-3472.
- [26] E.F. Murphy, L. Schmid, T. Bürgi, M. Maciejewski, A. Baiker, *Chem Mater*, 13 (2001) 1296-1304.
- [27] B. Tamami, S. Ghasemi, *Appl Catal A*, 393 (2011) 242-250.
- [28] D. Astruc, F. Lu, J.R. Aranzaes, *Angew Chem Int Ed*, 44 (2005) 7852-7872.
- [29] S. Roy, M.A. Pericas, *Org Biomol Chem*, 7 (2009) 2669-2677.
- [30] H. Veisi, M. Ghadermazi, A. Naderi, *Appl Organomet Chem*, 30 (2016) 341-345.
- [31] M. Kooti, M. Afshari, *Mater Res Bull*, 47 (2012) 3473-3478.

- [32] B. Abbas Khakiani, K. Pourshamsian, H. Veisi, *Appl Organomet Chem*, 29 (2015) 259-265.
- [33] F. Heidari, M. Hekmati, H. Veisi, *J Colloid Interface Sci*, 501 (2017) 175-184.
- [34] M. Pirhayati, H. Veisi, A. Kakanejadifard, *RSC Adv*, 6 (2016) 27252-27259.
- [35] H. Veisi, M. Pirhayati, A. Kakanejadifard, *Tetrahedron Lett*, 58 (2017) 4269-4276.
- [36] G. Chouhan, D. Wang, H. Alper, *Chem Commun*, 0 (2007) 4809-4811.
- [37] G. Dodi, D. Hritcu, D. Draganescu, R.D. Andrei, M.I. Popa, *Colloids Surf A*, 542 (2018) 21-30.
- [38] K. Can, M. Ozmen, M. Ersoz, *Colloids Surf B*, 71 (2009) 154-159.
- [39] K. Vishal, B.D. Fahlman, B.S. Sasidhar, S.A. Patil, S.A. Patil, *Catal Lett*, 147 (2017) 900-918.
- [40] V. Kandathil, B.D. Fahlman, B.S. Sasidhar, S.A. Patil, S.A. Patil, *New J Chem.*, 41 (2017) 9531-9545.
- [41] M. Esmailpour, A.R. Sardarian, J. Javidi, *Appl Catal A*, 445-446 (2012) 359-367.
- [42] A. Ghorbani-Choghamarani, Z. Darvishnejad, M. Norouzi, *Appl Organometal Chem*, 29 (2015) 170-175.
- [43] S.S. Behera, J.K. Patra, K. Pramanik, N. Panda, H. Thatoi, *World J Nano Sci Eng*, 02 (2012) 196-200.
- [44] X. Wang, R. Niessner, D. Knopp, *Sensors*, 14 (2014) 21535-21548.
- [45] J. Zhang, N. Gan, S. Chen, M. Pan, D. Wu, Y. Cao, *J Chromatogr A*, 1401 (2015) 24-32.
- [46] Q. Zhang, H. Su, J. Luo, Y. Wei, *Catal Sci Technol*, 3 (2013) 235-243.
- [47] E. Nehlig, B. Waggeh, N. Millot, Y. Lalatonne, L. Motte, E. Guenin, *Dalton Trans*, 44 (2015) 501-505.
- [48] V. Polshettiwar, R.S. Varma, *Org Biomol Chem*, 7 (2009) 37-40.

- [49] A.R. Hajipour, N.S. Tadayoni, Z. Khorsandi, *Appl Organometal Chem*, 30 (2016) 590-595.
- [50] Q. Du, W. Zhang, H. Ma, J. Zheng, B. Zhou, Y. Li, *Tetrahedron*, 68 (2012) 3577-3584.
- [51] H. Yang, Y. Wang, Y. Qin, Y. Chong, Q. Yang, G. Li, L. Zhang, W. Li, *Green Chem*, 13 (2011) 1352-1361.
- [52] A.S. Singh, R.S. Shelkar, J.M. Nagarkar, *Catal Lett*, 145 (2014) 723-730.
- [53] M. Esmaeilpour, J. Javidi, F.N. Dodeji, M.M. Abarghoui, *Transition Met Chem*, 39 (2014) 797-809.
- [54] M. Esmaeilpour, A.R. Sardarian, J. Javidi, *J Organomet Chem*, 749 (2014) 233-240.
- [55] Z. Zarnegar, J. Safari, *New J Chem*, 38 (2014) 4555-4565.
- [56] N. Yilmaz Baran, T. Baran, A. Menteş, *Appl Catal A*, 531 (2017) 36-44.
- [57] S. Das, S. Bhunia, T. Maity, S. Koner, *J Mol Catal A: Chem*, 394 (2014) 188-197.
- [58] X. Jin, K. Zhang, J. Sun, J. Wang, Z. Dong, R. Li, *Catal Commun*, 26 (2012) 199-203.
- [59] S. Sobhani, M.S. Ghasemzadeh, M. Honarmand, F. Zarifi, *RSC Adv*, 4 (2014) 44166-44174.
- [60] H. Liu, X. Xue, T. Li, J. Wang, W. Xu, M. Liu, P. Chen, Y. Wu, *RSC Adv.*, 6 (2016) 84815-84824.
- [61] D. Yuan, L. Chen, L. Yuan, S. Liao, M. Yang, Q. Zhang, *Chem Eng J*, 287 (2016) 241-251.
- [62] Q. Zhang, H. Su, J. Luo, Y. Wei, *Tetrahedron*, 69 (2013) 447-454.
- [63] M. Gholinejad, M. Razeghi, C. Najera, *RSC Adv*, 5 (2015) 49568-49576.
- [64] R.K. Sharma, Y. Monga, A. Puri, *J Mol Catal A: Chem*, 393 (2014) 84-95.
- [65] M. Islam, P. Mondal, A.S. Roy, K. Tuhina, *Transition Met Chem*, 35 (2010) 427-435.
- [66] S.M. Islam, A.S. Roy, P. Mondal, N. Salam, *Appl Organometal Chem*, 26 (2012) 625-634.

[67] S.-T. Yang, P. Shen, B.-S. Liao, Y.-H. Liu, S.-M. Peng, S.-T. Liu, *Organometallics*, 36 (2017) 3110-3116.

[68] M. Baron, E. Métay, M. Lemaire, F. Popowycz, *Green Chem*, 15 (2013) 1006-1015.

[69] M. Gholinejad, F. Zareh, C. Nájera, *Appl Organomet Chem*, 32 (2018) e3984.

ACCEPTED MANUSCRIPT

Graphical Abstract (Pictogram)



Research Highlights

- ❖ A new magnetic nanoparticle tethered Schiff base-palladium(II) was successfully synthesized.
- ❖ MNPs@SB-Pd nanomagnetic catalyst was fully characterized.
- ❖ MNPs@SB-Pd nanomagnetic catalyst exhibited efficient catalytic activity in Suzuki-Miyaura cross-coupling and reduction of nitroarenes reactions.
- ❖ MNPs@SB-Pd nanomagnetic catalyst can be reused at least 10 times without obvious change in the activity.

ACCEPTED MANUSCRIPT